# Dynamical Climatology

## An intercomparison of the Met O 11 N45 model and the Met O 20 11-level model on the Cyber 205

by

J. F. Dyson

DCTN 10

November 1984

Meteorological Office (Met. O. 20)
London Road
Bracknell
Berkshire RG12 2SZ

DYNAMICAL CLIMATOLOGY TECHNICAL NOTE NO. 10

# AN INTERCOMPARISON OF THE MET O 11 N45 MODEL AND THE MET O 20 11 LEVEL MODEL ON THE CYBER 205

by

J F DYSON

Met O 20 (Dynamical
Climatology Branch)
Meteorological Office
London Road
Bracknell
Berkshire, U.K. RG12 2SZ

November 1984

# AN INTERCOMPARISON OF THE MET O 11 N45 MODEL AND THE MET O 20 11 LEVEL MODEL ON THE CYBER 205

BY J F DYSON

## 1. Introduction

This paper is a report on a comparison between the N45 model[1] and the Met O 20 model[2]. The essential difference between the two models is in the dynamics. The N45 model uses a split explicit scheme (Gadd 1978, Davies 1980) whereas the Met O 20 model uses a leap frog scheme (Saker 1975).

The potential advantage in using the N45 model is the reduced memory requirement; because the split explicit dynamics requires only one time level the memory required is virtually half that used by the leap frog scheme. This would allow more room for diagnostics and/or a finer resolution version. For the configurations described in table 1 the N45 model uses 75 seconds CPU time, 150 seconds elapsed for 1 day of model integration; the corresponding figures for the Met O 20 model are 160 seconds and 290 seconds. Almost all the differences in CPU time are because the Physics routines are called three times as often in the Met O 20 model. The extra difference in the elapsed time is due to the extra diagnostic facilities used in the Met O 20 model. Thus, although the N45 model would be marginally faster, the main advantage of using it would be because of its reduced memory requirement.

Of course there would be no point in Met O 20 adopting the N45 model if its simulation of the climate were considerably worse than the Met O 20 model's simulation. We have chosen two criteria for the comparison, one subjective

---

[1]Definitions for the purpose of this paper:

'N45 model' = Met O 11's 11 level global (128 x 91 grid points) version of the Cyber forecst model with Physics routines as described in Table 1.

[2]

'Met O 20 model' = 11 level 2° x 3° version of the Met O 20 Cyber model with Physics routines described in Table 1.

and one numerical. The subjective criterion used is comparing the response to fixed external forcing for January and June conditions. The numerical criterion chosen was to study the mass and moisture conserving properties of the two models.

In Section 2 the climatologies of the two models are compared and contrasted with observations on the basis of one June and one January integration. In Section 3 the mass and moisture budgets are compared and conclusions are drawn in Section 4.

## 2. Comparison of the Simulated Climatologies

A comparison of the characteristics of the two models is presented in Table 1.

Table 1: Comparison of Model Characteristics

| Model | N45 | Met O 20 |
|---|---|---|
| Grid Type | Regular Lat-Long Arakawa B | Regular Lat-Long Arakawa A |
| Resolution | 2° x 2.81° (91 x 128 points) | 2° x 3° (90 x 120 points) |
| Dynamics | Split Explicit (without virtual temperature effects) | Flux form 2nd order centred differences with a leap frog timestep (without virtual temperature effects) |
| Timestep | 20 min (this is the advection timestep and time between calls to Physics routines) | $7^1/_2$ min (this is the time-step between calls to Physics routines; the leap-frog timestep is 15 min) |

| | | |
|---|---|---|
| Noise Filter | Non linear diffusion of u, v θ and q in σ surfaces in the bottom 4 σ-surfaces in p surfaces elsewhere; diffusion constant = $10^{15}m^3$ (u,v), $m^4s^{-1}K$(θ), $m^4s^{-1}$ (q) | Non linear diffusion of u, v and θ in σ-surfaces diffusion constant $10^{15}m^3$ (for u, v) $m^4s^{-1}K$ for θ linear diffusion of q with constant $10^4$ ($m^2s^{-1}$) |
| Stability Filter | Fourier chopping | Multipoint Filter |
| Boundary Scheme | Richards | Richards |
| Radiation | Climatological | Climatological |
| Evcon | 9 | 9 |

Evcon is a parameter which appears in the convection routine. It controls the rate at which precipitation evaporates as it falls. Increasing it has a considerable effect on the precipitation distribution (Rowntree 1984). It is worthy of note that the physics routines are called $2^2/_3$ times as often in the Met O 20 model as in the N45 model. However the main differences are in the dynamics and filtering routines, both stability and noise.

## 2a. The January Integrations

DCRX3 was a 42 day January climatological integration of the N45 model and DC8E was a 42 day January climatological run of the Met O 20 model. The initial data for both runs were derived from day 8 of HGC4[1]. Means of the last thirty days of each integration were used as the basis of the comparison.

Figure 1 shows the zonal mean PMSL plots for DC8E, DCRX3, Schutz and Gates climatology and FGGE data meaned over January 1979. The most striking feature is that DCRX3 and DC8E are much closer to one another than either is to Schutz and Gates climatology or FGGE data - at least north of 60°S.

[1]Unfortunately there are differences in the initial soil moisture field. In DC8E the initial data were interpolated from the IBM 11 level Kurihara grid. The soil moisture content was set to 5 cm if the interpolated result was greater than zero and zero otherwise. DCRX3 has initial data with a more realistic SMC field. These differences may affect precipitation over land, particularly over deserts.

This is particularly true in northern mid latitudes where both models over-emphasize the trough at 60°–70°N (NB neither model has the so-called 'over deepening' correction to the boundary and convection scheme[1] (Cullen 1982)). DCRX3 produces 988 mb, DC8E (990 mb) as against Schutz and Gates climatology (1014.5 mb) and FGGE (1014 mb). In southern mid-latitudes, however, DC8E does not produce a deep enough Antarctic trough. On the other hand DCRX3 has a similar minimum to Schutz and Gates (within 2 mb). At the time of writing no quantitative determination of the Met O 20 models' variability has been made, but ten day zonal means (Figure 2) and the results shown by Rowntree and Mitchell (1982) suggest that the differences between the climatological and model data sets are unlikely to have occurred by chance.

Both DCRX3 and DC8E produce Icelandic lows of 972 mb (see Figures 4 and 5) compared to the climatological 1000 mb (Figure 3). Relative to the climatology both runs have the Azores high shifted eastward over the Sahara. Both models have the Siberian high displaced southward to 45°N with a central value of about 1032 mb. The equatorial trough – as defined by the 1008 mb contour – is similarly placed in both integrations and close to the climatological position. The maximum pressure at 60°N in the north American ridge is about 996 mb in DCRX3, 1010 mb in DC8E and 1022 mb in the climatology. On this criterion DCRX3 is simulating the climatology worse than DC8E. In both runs the mid latitude zonal flow is too strong. The values for the globally averaged kinetic energies (KE) bear this out. In Table 2 $K_S$ is the standing eddy KE, $K_T$ the transient eddy KE, $K_Z$ the zonal and K the total KE all meaned over the last thirty days of the experiments (this terminology is as in Table 4 of Rowntree and Mitchell 1982; note $K_E = K_T + K_S$).

---

[1]Very recently the N45 model has been run with a $7^1/_2$ min timestep and from the same initial data as DCRX3. The minimum in the Northern Hemisphere trough is 991 mb. Some of the differences between DCRX3 and DC8E, therefore, may be explained by the difference in the timestep.

Table 2: Global KE for DCRX3 and selected January Met O 20 runs

Units J/Kg ($M^2s^{-2}$)

| | Experiment | K | $K_Z$ | $K_S$ | $K_T$ | $K_E/K$ |
|---|---|---|---|---|---|---|
| | DCLC | 180 | 102 | 37 | 41 | .43 |
| | DC8K | 194 | 97 | 32 | 65 | .50 |
| | DC8E | 182 | 105 | 36 | 40 | .42 |
| | DCRX3 | 206 | 126 | 27 | 53 | .38 |
| MO3A | FGGE - JAN+ | 150 | 76 | 20 | 54 | .49 |
| | FGGE - FEB+ | 147 | 75 | 18 | 54 | .49 |
| EC3B | FGGE - JAN+ | 162 | 81 | 19 | 61 | .50 |

+ Omitting 0–50 mb

The time evolutions of the globally averaged zonal and eddy KE's for each run are shown in Figure 6. DC8E appears to be relaxing towards an equilibrium after increasing for the first 25 days. However in DCRX3 $K_Z$ keeps increasing; DCRX3 has been run on for another 20 days and the trend continues upward. At day 62 the $K_Z$ is 156 $m^2s^{-2}$ with no sign of a steady state having been reached. This ties in with Figure 2a which shows the ten day means of the zonally averaged PMSL field for DCRX3. As time goes on the northern mid latitude trough becomes deeper and deeper. This is not the case for DC8E (Figure 2b). This suggests that excessive westerly flow is a more serious problem in the N45 model than in the Met O 20 model.

Figure 7a and 7b show the westerly wind field, zonally averaged, in a height latitude cross-section for DC8E and DCRX3. Figure 7c shows the same for January FGGE data. Comparing the relative strength of the mid latitude tropospheric jets we see that in DC8E there is a maximum of 42.3 $ms^{-1}$ at (33°N, 240 mb) whereas in DCRX3 the jet is not closed off but has a maximum of about 45 $ms^{-1}$ at 55°N above 100 mb. In the FGGE data for January the maximum is 38.9 $ms^{-1}$ at (30°N, 200 mb). Thus DC8E represents this feature much better than DCRX3. In the southern hemisphere FGGE data places the southern mid tropospheric jet at (50°S, 250 mb) with a value of 33.8 $ms^{-1}$. Both DC8E and DCRX3 position the jet maximum at (43°S, 250 mb) with values of 33.9 $ms^{-1}$ and 31.1 $ms^{-1}$. Bearing in mind the fact that the FGGE year was exceptional (Trenberth 1984) it cannot be concluded that either model is superior in this respect. Both models have the tropical easterlies too strong reaching 8 $ms^{-1}$ against 5 $ms^{-1}$ in the FGGE data. DCRX3 deviates enormously from FGGE in the southern hemisphere stratosphere where easterlies extend from the south pole to the equator above 100 mb with values in excess of 25 $ms^{-1}$. DC8E is much closer to FGGE in this respect.

The zonally averaged temperature in height latitude cross-section for DC8E, DCRX3 and January FGGE data are shown in Figure 8a, 8b and 8c. Note the 'hot spot' of over 260°K in DCRX3 in the south polar stratosphere. This is consistent with the excessive stratospheric easterlies described above. The time evolution of this warming has been investigated. It was found that most of the heating was confined to the $\sigma$ level second from the top of the model atmosphere ($\sigma$ = .089) and (to a lesser extent) those above and below, and from 90°S to 45°S. The zonally averaged temperature at (78°S, $\sigma$ = .089) reaches a maximum on day 15 of 278K (228Kin the initial data). This suggests that the stability filter (the N45 model is filtered from 90°s to 45°S) may be playing a role in the warming. The N45 model was run for 10 days from the same initial conditions but with diffusion on $\sigma$-surfaces at all levels and the same rapid warming occurred (in fact slightly more over these 10 days), suggesting that the form of diffusion used is not responsible for the warming observed. Note the anomalously high temperatures seen in these cross sections near the surface in northern latitudes. This does not reflect the actual temperatures produced by the model but is an artifact of interpolating from $\sigma$ to pressure surfaces when plotting these cross sections.

Elsewhere in the troposphere the differences (Fig 8d) are less than 2K below 500 mb and at most 5K below 200 mb (except in the Antarctic stratosphere as discussed above). The differences in the globally averaged density weighted atmospheric temperature for which DCRX3 is 2.25K warmer than DC8E are mostly accounted for in the differences in the stratosphere.

Figures 9a, b and c show surface temperatures for DC8E, DCRX3 and the difference between them. The differences seen in surface temperature over Southern Asia, Africa and South America are probably due to the differences in the Soil Moisture content (Figures 10a, b, c)) which reflect the differences in the initial soil moisture. The differences in surface temperature in Canada are consistent with the surface winds (Figures 4 and 5) in that in DCRX3 more heat is advected from the Ocean (effectively the Ocean is an infinite heat source (or sink) because of the fixed sea surface temperatures) than in DC8E. Over Eastern Russia the colder surface temperatures in DCRX3 probably reflect the fact that the low level winds are more northerly than in DC8E.

We now consider the precipitation fields produced by the two models. Both DCRX3 and DC8E produce global mean values of 3.45 and 3.26 mm day$^{-1}$ respectively for the thirty day means. These may be compared with the estimates of Jacobs (1968) of 2.94 mm day$^{-1}$ for January and Jaeger (1976) of 2.65 mm day$^{-1}$ for the same period. In the zonal mean (Figure 11) both produced peaks at 10°S with 9.1 mm day$^{-1}$ for DCRX3 and 8.45 mm day$^{-1}$ for DC8E. In contrast both the climatological estimates shown in Figure 11 have local maxima at 6°S with a value of 5.3 mm day$^{-1}$ (Jacobs) and at 7°S with a value of 4.9 mm day$^{-1}$ (Jaeger). In the case of Jaeger this is the maximum zonal mean. Jacobs gives a maximum of 5.75 mm day$^{-1}$ at 7°N. DC8E simulates this feature well with a local maximum of 5.25 mm day$^{-1}$ at 5°N. DCRX3 has a less pronounced local maximum of 4.70 mm day$^{-1}$ at 7°N, nearer to the value given by Jaeger of 4.8 mm day$^{-1}$ at 2°N. In DC8E the equatorial minimum is more pronounced than either of the climatological estimates. In contrast DCRX3 has a local minimum at 2°N with values only slightly below the two climatological estimates. The local minimum at 20°N seen in both climatologies is reproduced in both runs. Neither model reproduces the large local maximum at 60°S seen in Jaeger's climatology but absent from Jacobs'. In summary both reproduce the main climatological features with the exception of producing too large a maximum at 10°S. DC8E produces values generally closer to climatology than DCRX3 but the difference is slight.

The global precipitation patterns are shown in Figures 12 and 13 with climatology shown in Figure 14. The shaded areas - mean precipitation greater than 5 mm $day^{-1}$ - show a broadly similar structure in both runs. There are some differences, however, in positioning and intensity. For example DC8E has more intense rainfall over Brazil and in the south Atlantic off the coast of Brazil. The band of precipitation in the neighbourhood of the equatorial Atlantic - the models' simulated ITCZ - is positioned on and just south of the equator in DC8E and just north of the equator in DCRX3. In the Indian Ocean the region with rainfall greater than 5 mm $day^{-1}$ extends from Africa over Indonesia and into the Pacific in DCRX3, whereas in DC8E in the eastern Indian Ocean there is considerably less precipitation. In general in the tropics precipitation in DCRX3 is more widespread and less intensely localized.[1] The global maximum for DC8E is 56 mm $day^{-1}$ at 163 E, 9°S and for DCRX3 40.5 mm $day^{-1}$ at 163°E, 10°S. In relation to climatology the intense rainfall along the ITCZ is more faithfully reproduced by DCRX3 - particuarly in the Indian Ocean. The areas of low precipitation in the southern oceans, as judged by the 1 mm $day^{-1}$ contour, are well represented by both models. In the Pacific, just off the south west of Mexico, both models have a local maximum of 20 mm $day^{-1}$ a feature not seen in the climatology. It is associated with a local maximum in the sea surface temperature. Both models overestimate, by a factor of two the rainfall associated with the north Atlantic and north Pacific depression belts. This is consistent with the excessive depth of these deprssion belts (Figures 3-5). The roughness in the precipitation north of 60°N and south of 60°S in DCRX3 is believed to be associated with the type of filtering used. In the fine mesh forecast model a similar precipitation pattern was observed when Fourier filtering was being used and was removed with the introduction of the multipoint filter.

---

[1]The differences in the Initial soil moisture fields are probably at least partially responsible for the differences in rainfall over equatorial Africa seen in the 30 day mean. They could have some effect on the extra-tropical circulation.

## 2b. The June Integrations

The N45 model integration DCRX1 and the Met O 20 2° x 3° integration DC11 both started from the same initial data JUNIDATA (which was derived from the operational analysis for June 27th 1983) and use June SST and July radiationconditions. The means of the last 30 days of the 50 day integrations are compared here with July FGGE data and Schutz and Gates climatology although a June comparison might be more appropriate in view of the SST's.

The zonal means of the PMSL fields for DC11 and DCRX1 are plotted in figure 15 together with Schutz and Gates July climatology and FGGE data for July 1979. The climatological trough at 65°N is about $1^1/_2$ mb deeper in DCRX1 than in both the climatologies; DC11 reproduces this feature more faithfully, although this is probably within the noise level of the model integrations. From 60°N to 20°S both DC11 and DCRX1 are close to the climatologies although it should be noted that in the tropics DCRX1 is up to 2 mb lower than DC11 (DC11 lies between the climatologies). DCRX1 is about 4 mb too high at the southern sub-tropical ridge; DC11 is also too high but less so. DC11 has the Antarctic trough close to the FGGE value at 975 mb (FGGE 980 mb) although the tailing off of pressure south of this is unrealistic but characteristic of Met O 20 northern summer runs. (It should be noted here that Trenberth's (1984) analysis of station data shows that the July 1979 pressures were exceptionally low in this area). In DCRX1 the Antarctic trough is a more well defined feature but its minimum is nearly 10 mb deeper than FGGE [NB south of 75°S comparisons are dubious because of the high topography].

Figures 16 to 18 show PMSLfields for DC11, DCRX1 and Schutz and Gates July climatology respectively. In the less active northern hemisphere the two runs are very similar. In both integrations the intensity of the Azores high is close to climatology. Because of the positioning of the Azores high, however, neither model reproduces the westerly flow over the British Isles seen in the climatology. The north Pacific high, as delineated by the 1024 mb contour, is too elongated in both integrations. The monsoon low, as defined by the 1000 mb contour, is well reproduced in both runs.

As seen in the zonal mean (fig 15) DCRX1 produces too low a pressure along the equator particularly in the Indian Ocean. The southern sub-tropical ridge, as defined by the 1020 mb contour, (see also fig 15) is stronger than observed in both DCRX1 and DC11 in the Eastern and Western Pacific and in the southern Atlantic. Over southern Africa and the Indian Ocean the sub-tropical ridge is too weak in DC11 but again too strong in DCRX1. The westerly flow around the southern oceans is too intense in both models, with DCRX1 having the tighter gradients (this is borne out by the ZKE of DCRX1 in the band 30°S to 90°S of 305 $m^2s^{-2}$ against 267 $m^{-2}s^{-2}$ for DC11). Both runs produce minima of less than 968 mb off the Antarctic coast well below this climatological minimum of about 980-985 mb. In summary: both models reproduce the norhtern hemisphere PMSL patterns reasonably well. The southern sub-tropical high is over-emphasized in both runs, particularly DCRX1, and mispositioned in both. DCRX1 over-emphasizes the Antarctic trough relative to both FGGE data and Schutz and Gates climatology. DC11 is closer to FGGE in this respect - at least in the zonal mean.

The zonal, standing eddy and transient eddy kinetic energies are shown in table 3. Again the terminology is as in Rowntree and Mitchell (1982).

Table 3: Global K.E. for June and July for DCRX1, selected Met O 20 runs and July FGGE data.

| | K | $K_Z$ | $K_S$ | $K_T$ | $K_E/K$ |
|---|---|---|---|---|---|
| DCAC | 161 | 100 | 21 | 40 | .38 |
| DCAD | 156 | 98 | 24 | 34 | .37 |
| DCAK | 178 | 102 | 21 | 55 | .43 |
| DCJK | 177 | 102 | 24 | 51 | .42 |
| + DC11 | 161 | 115 | 15 | 31 | .29 |
| + DCRX1 | 157 | 112 | 16 | 28 | .28 |
| x MO3A FGGE July | 133 | 74 | 14 | 44 | .43 |
| x EC3B FGGE July | 137 | 75 | 13 | 49 | .45 |

+ June SST's: July radiation

x Omitting 0-50 mb (see Tech Note 204)

The most obvious feature of this table is how similar DC11 and DRCX1 are in the partitioning of the Global Kinetic energy. Compared to the July FGGE analyses (both MO3A and EC3B) the zonal kinetic energy is too high and the transient eddy kinetic energy too low in both runs. Note that the difference in transient eddy K.E. between the N45 and the Met O 20 models in the January runs is far larger than in the June runs and of opposite sign. The ratio of total eddy K.E. to total K.E. is too low in both runs. The zonal K.E. is slightly higher in DC11 than in DCRX1; however, as mentioned above, the zonal kinetic energy in the band 30°-90°S is considerably higher in DCRX1 (305 $m^2s^{-2}$ vs 267 $m^2s^{-2}$) reflecting the deeper Antarctic trough seen inthe zonal PMSL for DCRX1 (fig 15). Figure 19 shows the time evolution of zonal and eddy kinetic energy. Unlike the January runs the N45 run appears to have reached an equilibrium in zonal kinetic energy at a similar level to DC11's. The eddy kinetic energies are also similar, oscillating about a similar mean but with a different phase.

Figures 20a, b and c show height-latitude cross-sections of zonally meaned westerly wind for DCRX1, DC11 and July FGGE (EC3B analysis) respectively. Taking the intersection of the 10 $ms^{-1}$ contour with 950 mb as an indicator of the surface westerly flow in southern mid-latitudes, we see that in DCRX1 this area stretches from 44°S to 62°S, in DC11 from 45°S to 59°S and in July FGGE from 49°S to 62°S. Thus by this measure the surface westerlies are excessive in DCRX1 and too far north in DC11. Both models simulate well the overall structure and intensity of the southern mid-latitude tropospheric jet. The northern mid-latitude tropospheric jet is too far south in DCRX1 but the strength is correct; DC11 positions the jet well in terms of latitude but a little low and the strength of the jet is slightly less than the FGGE data. The easterlies in the tropical stratosphere are too strong in both models.

Figure 21a, b and c show height-latitude cross-sections of zonally meaned temperature for DCRX1, DC11 and July FGGE data. Fig 21d shows the difference between DC11 and DCRX1. As in the January case the largest differences are in the stratosphere. (The low stratosphere ($\sigma$ = .022) temperatures in DC11 and DC8E are due to diffusion on $\theta$ surfaces. Diffusing a linear combination of $\theta$ and T cures this to a large extent (see fig 6 of Rowntree and Mitchell)). DCRX1 gives a much more faithful representation of the tropopause than DC11 when compared with FGGE July. Again, as in the January case, the horizontal interpolation of fields on pressure surfaces means that spuriously high temperatures, which are not actually in either model appear in these cross-sections near the surface in high latitudes. Large differences, however, are seen over Antarctica between both model runs and FGGE July data. For example at 600 mb at the South Pole both models are nearly 10 K colder than FGGE, though the difference is quite local with similar temperatures at 70°S.

The zonally averaged total precipitation for DCRX1, DC11, Moller's July climatology and Jaeger's June climatology are shown in figure 22. Both runs produce excessive amounts of precipitation in the global average with respect to both climatological estimates. DC11 produces 14% and DCRX1 16% above Jaegers (the more recent) estimate of the global mean. The zonal means in the two runs are very similar. Both have a spurious maximum at

65°N, when compared to the two climatologies. There is another spurious feature, at about 7°S, common to both runs. Elsewhere both runs have a similar qualitative structure to the climatologies but in general the values are about 15% larger.

Figures 23a, b and c show the total precipitation fields for DCRX1 and DC11 and the difference between the two. Figures 24a and b show the climatologies of Moller and Jaeger. The most striking feature, at least to the eye, is how similar the two runs are. The difference chart seems to suggest otherwise. However, for example, in the central southern Pacific the shaded area in DC11 (>5 mm $day^{-1}$) is of similar shape to but slightly smaller than the shaded area in DCRX1 but positioned to the north of it. In general although the overall pattern looks similar the difference chart shows that the positions of the precipitation bands are shifted. When compared to climatology the large spurious maximum at 65°N in the zonal mean is manifested as excessive precipitation over North America and Siberia in both runs. The spurious maximum at 7°S in the zonal mean is accounted for by excessive (as delineated by the >5 mm/day area) rainfall in the central Pacific and Indian Ocean. It is quite possible that Jaeger has got the Indian Ocean intensity wrong here; Jaeger's S.E. Pacific data is probably closer to reality because of the higher density of land data. Neither Moller nor Jaeger show an area of greater than 5 mm/day in the south east Pacific whereas both models do. Jaeger has an area of greater than 5 mm/$day^{-1}$ south of the equator in the Indian Ocean but of much lesser extent than either model. Moller does not show any here. The area of high precipitation associated with the Monsoon low extends too far westward from India in both models when compared to Moller but is in reasonable agreement with Jaeger. In DC11 it does not extend into the west Pacific as is seen in the climatologies. In this respect DCRX1 is in much better agreement with the climatologies. As in the January run DCRX1 is afflicted by gridscale roughnesses in the precipitation field in high latitudes.

To summarize: these two runs are much closer to one another than the January runs are to each other. But as in the January cases the two runs were much closer to one another than to the observed climatology.

### 3. Mass and Moisture budgets

When doing long term climate studies, as opposed to a ten day forecast say, it is important that quantities conserved (locally or globally) in nature - or rather by the continuous system of equations - should be conserved as closely as possible by our discrete model. These quantities include total mass, water content and total energy. Construction of an energy budget would have required the development of more diagnostics than seemed justified for this study. Accordingly only a mass and moisture budget have been done.

DCRX3 loses .038 mb day$^{-1}$ over the last 30 days compared to .0012 mb day$^{-1}$ for DC8E (DC8E is typical of Met O 20 runs in that other January Cyber integrations also lose less than .01 mb day$^{-1}$). For the June runs, when averaged over the last 30 days of each run, DCRX1 loses .015 mb day$^{-1}$ whilst, in contrast, DC11 loses less than .005 mb day$^{-1}$. These differences are presumably due to the form of the N45 model dynamics which are not written in flux form. Attempts have been made (Duffy 1981) to write the split explicit scheme in flux form but this variant of the scheme became rapidly unstable. Another possible factor in the difference in the rate of mass loss between the two schemes is in the stability filtering. In the N45 model PMSL is filtered (inherently non conservative) whilst in the Met O 20 model the $p_*$ increments are filtered.

The N45 model also performs less well at moisture conservation. Not only is the moisture advection equation not written in flux form but the diffusion of specific humidity inthe N45 model is non linear as opposed to linear in the Met O 20 model. Another important difference between the models is the treatment of negative specific humidity when it occurs. In the N45 model if a negative specific humidity is produced at a point it is set to zero. This is effectively a spurious source of moisture. In the Met O 20 model if a negative specific humidity appears in a grid box then the fluxes of moisture to and from the neighbouring grid boxes are set to zero at the next timestep if (and only if) their effect is to make the humidity more negative. This procedure is conservative. To give a fairer comparison between the models a mass weighted global mean of negative humidity (ie the total source of moisture attributable to the zeroing of negative specific humidity) meaned over each day was computed and included in the budgets for the N45 model (referred to as A.N.H. or accumulated negative humidity).

Table 4: Global moisture budget: meaned over last 30 days (mm day$^{-1}$)

| Experi- ment | Precipi- tation (P) | Evapor- ation (E) | E-P | A.N.H. | A.N.H. + (E-P) | Change in global q | Discrep- ancy |
|---|---|---|---|---|---|---|---|
| DC8E | 3.25 | 3.20 | -.05 | n/a | n/a | -.05 | <.01 |
| DCRX3 | 3.45 | 3.13 | -.32 | .18 | -.14 | -.04 | .10 |
| DC11 | 3.38 | 3.32 | -.05 | n/a | n/a | -.06 | .01 |
| DCRX1 | 3.45 | 3.26 | -.19 | .16 | -.03 | -.03 | .01 |

Two points arise from this table. First note the enormous improvement taking A.N.H. into account makes for DCRX1 and to a lesser, but still considerable, extent for DCRX3. When it is taken into account the discrepancy is reduced from .32 to .10 mm day$^{-1}$ for DCRX3 and from .16 to less than .01 mm day$^{-1}$ for DCRX1. (Since writing the first draft the January run of the N45 model has been re-run with a $7^1/_2$ min timestep; the discrepancy in this case was .025 mm day$^{-1}$ 75% down on the 20 min timestep). The second point is that DC8E is still considerably better, in this respect, than DCRX3 with a discrepancy of .0012 mm day$^{-1}$ (cf table 8 of Rowntree and Mitchell Tech Note 194). The discrepancy in DCRX3 is consistent through the last 30 days being roughly the same for each of the three ten day periods which make up the last 30 days.

## 4. Conclusions

In terms of the simulated climatology the main conclusion, on the basis of these two experiments, is that the two models are much closer to one another than to climatology. The main differences are summarized in table 5. In the case of the June runs it is not possible to select one in preference to the other. However in the January case there is some evidence that the Met O 20 model run performs better in that the N45 run does not approach equilibrium in Zonal Kinetic Energy[1] and, associated with this, the surface westerlies in northern mid-latitudes are more intense in DCRX3 than in DC8E. Allowance for the atypical nature of FGGE July would suggest that the N45 model has a similar problem in the southern winter though perhaps not worsening with time. The roughness seen in high latitudes in the precipitation field in the N45 runs are probably due to the Fourier filtering employed in the model. The evidence for this is that the Fine mesh forecast model exhibited this feature when Fourier filtering was used but the precipitation field became smoother when a multipoint filter was employed instead.

For use as a model in climate simulations the N45 model does appear to have some drawbacks when compared to the Met O 20 GCM. Firstly the N45 model is not as good at conserving mass. It is possible that a change in the stability filtering in the N45 model might improve this. A harder problem to overcome would be the N45 models failure to conserve moisture. Firstly a more realistic way of dealing with negative humidity would be needed. Even if this were achieved the results of the moisture budgets suggest that the N45 model can be (ie in the January case) unexpectedly bad in conserving total water content. To improve it further would probably require a fairly drastic reformulation of the split explicit scheme.

---

[1] The $7^1/_2$ min timestep run of the N45 model also suffers from this fault although the growth rate of Zonal Kinetic Energy is less (see DCRX4 in figure 6).

Table 5: Summary of the main differences between the N45 model and the M O 20 model.

| | N45 better | Met O 20 better |
|---|---|---|
| JAN | Antarctic trough | North American Ridge |
| | $K_T$ | N.H. Jet structure |
| | | S.H. Stratosphere |
| | | $K_Z$ |
| | | (in particular the non equilibrium of $K_Z$ in the N45 model) |
| JUNE | Tropopause (but a $T+b\theta$ diffusion corrects this defect in the Met O 20 model) | S.H. Westerlies |

## 5. Acknowledgements

I would like to thank Dr Mitchell and Dr Rowntree for the help and encouragement given in the preparation of this technical note.

## References


| | | |
|---|---|---|
| Cullen, M.J. | 1982 | Met O 11 Working Paper No 33 |
| Cunnington, W.M. | 1979 | Met O 20 Technical Note No II/138 |
| Davies, T. | 1980 | Met O 11 Working Paper No 18 |
| Duffy, D.G. | 1981 | A split explicit reformulation of the regional numerical weather prediction model of the Japan Meteorological Agency, MWR, Vol 109, No 5, pp 931-945 |
| Gadd, A.J. | 1978 | A split explicit integration scheme for numerical weather prediction Q.J.R.M.S., 104, p 569 |
| Gadd, A.J. | 1978 | A numerical advection scheme with small phase speed errors, Q.J.R.M.S., 104, p 583 |
| Jacobs, W.C. | 1968 | The Seasonal Apportionment of Precipitatin over the Ocean. Year-book of the Association of Pacific Coast Geographics, Vol 30, pp 63-78 |
| Jaeger, L. | 1976 | Monatskarten des Niederschlags fur die ganze Erde. Bericht Deutsche, Wetterdienst, 18, No 139 |
| Oort, A.H. and Rasmusson, E.M. | 1971 | Atmospheric Circulation Statistics NOAA professional paper No 5 |

| | | |
|---|---|---|
| Rowntree, P.R. | 1984 | Met O 20 Technical Note No II/226 |
| Rowntree, P.R. and Mitchell, J.F.B. | 1983 | Met O 20 Technical Note No II/194 |
| Saker, N.J. | 1975 | An 11 level General Circulation Model Met O 20 Technical Note No II/30 |
| Swinbank, R. | 1980 | Met O 20 Technical Note No II/151 |
| Trenberth, K.E. | 1984 | Interannual Variability of the Southern Hemisphere Circulation: Representativeness of MWR, Vol 112, No 1. |

Figure 1 Zonal mean PMSL (January case)
DCRX3 mean of days 13 to 42 . . . . .
DC8E """""""""""""""""""""""" × × × ×
Schutz & Gates climatology ⊙⊙⊙⊙
FGGE data for January + + + +

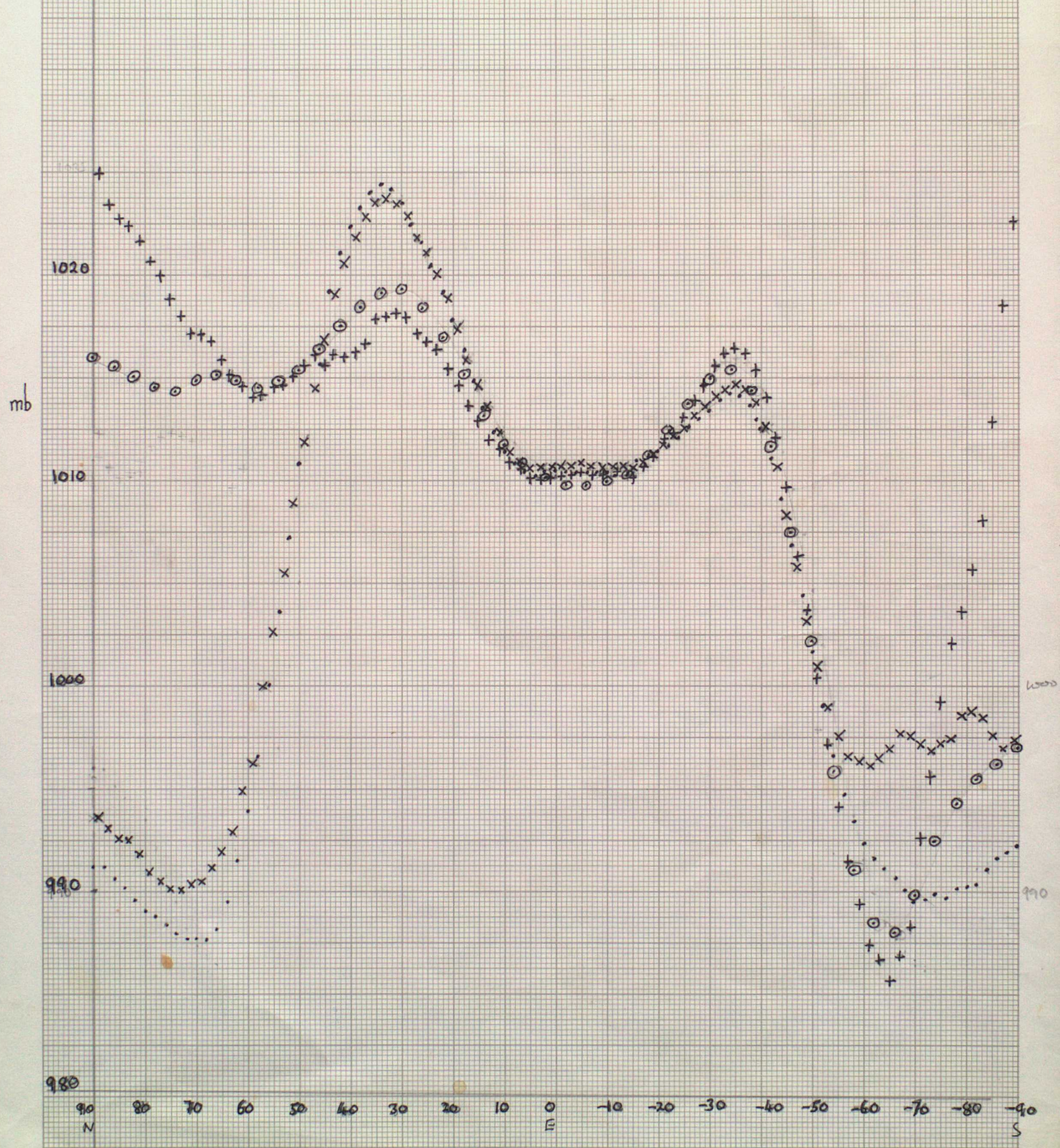

Figure 2a  Zonal mean PMSL for ten day means from DCRX3
days 13-22 + + + +
days 23-32 × × × ×
days 33-42 · · · ·

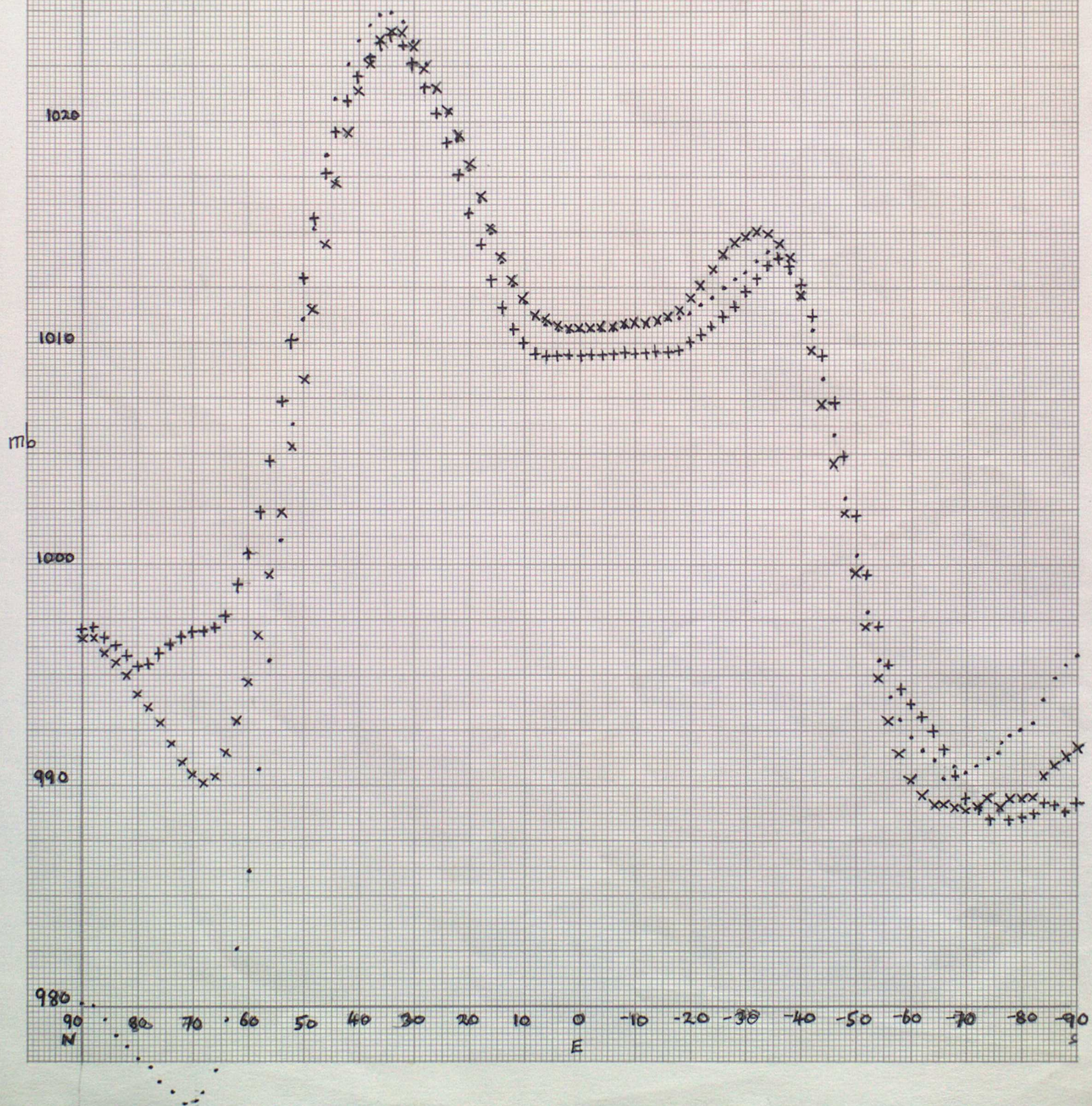

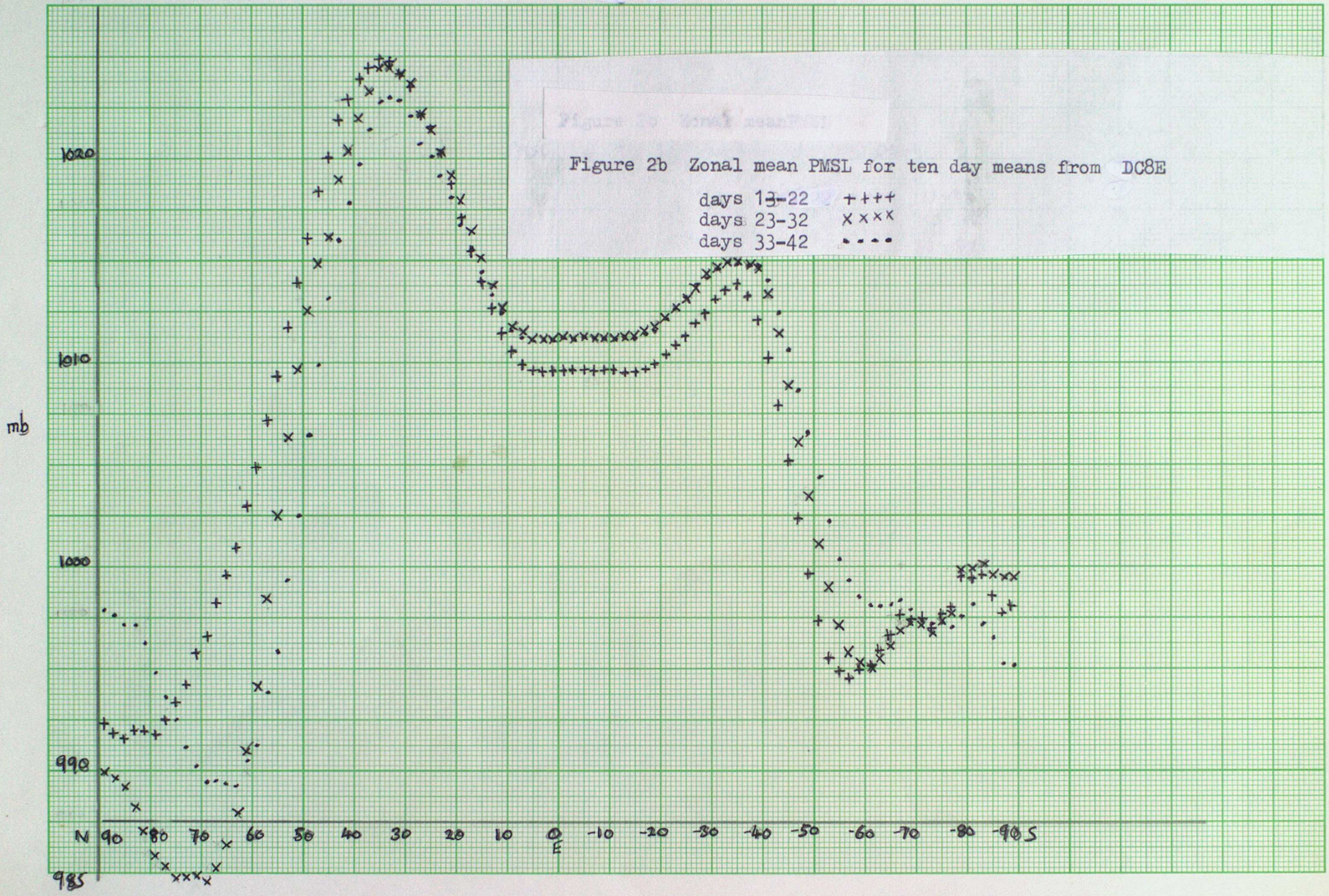


Figure 2b Zonal mean PMSL for ten day means from DC8E

Figure 3

SCHUTZ AND GATES DATA
JANUARY PMSL
AVERAGE FROM 0Z ON 1/1 DAY 1 TO 0Z ON 31/1 DAY 31
LEVEL: SEA LEVEL

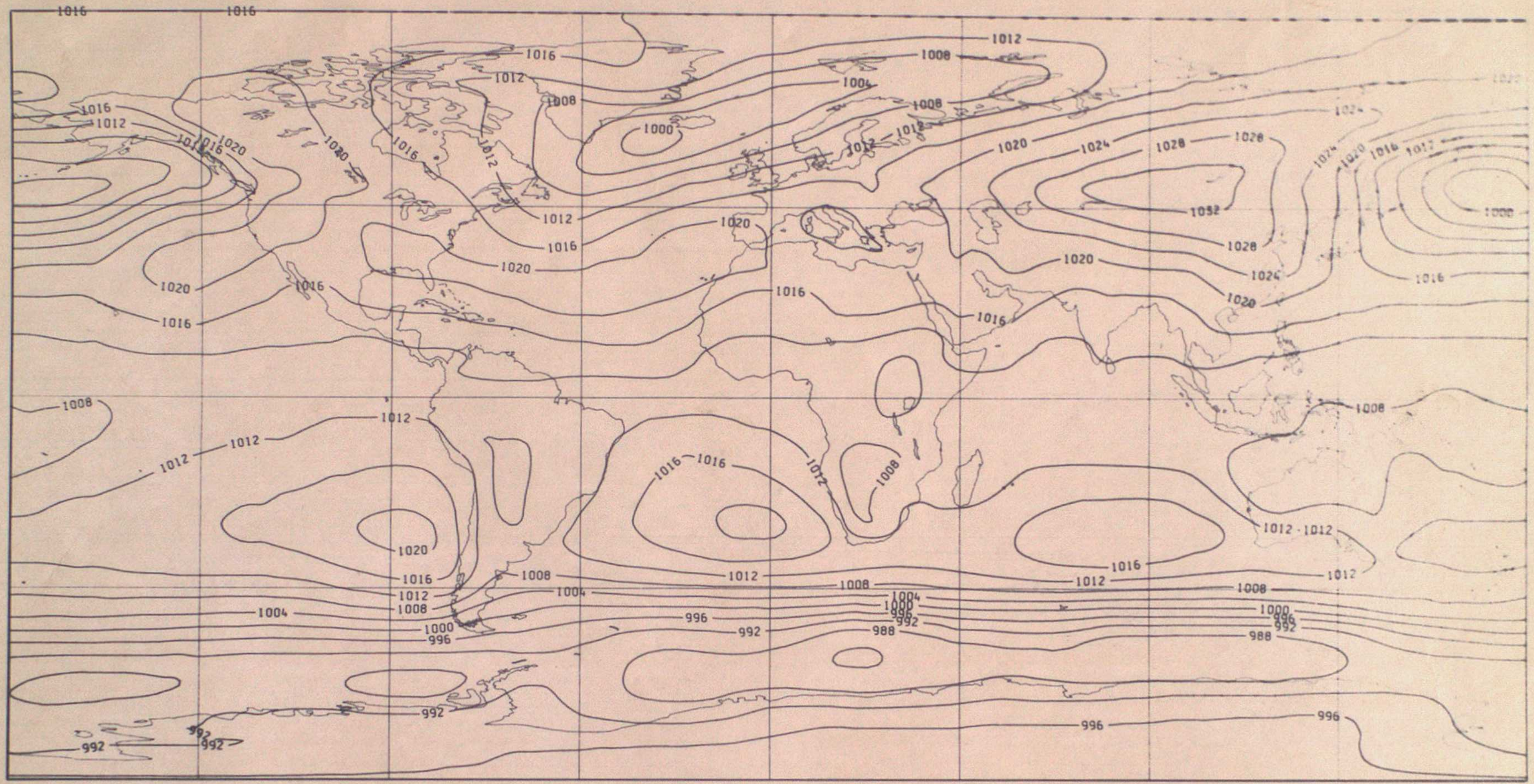

Figure 4

DCRX3M13    MSL PRESSURE    (MB)
ISOBARS EVERY 4MB
VALID AT 0Z ON 13/0
LEVEL: SEA LEVEL

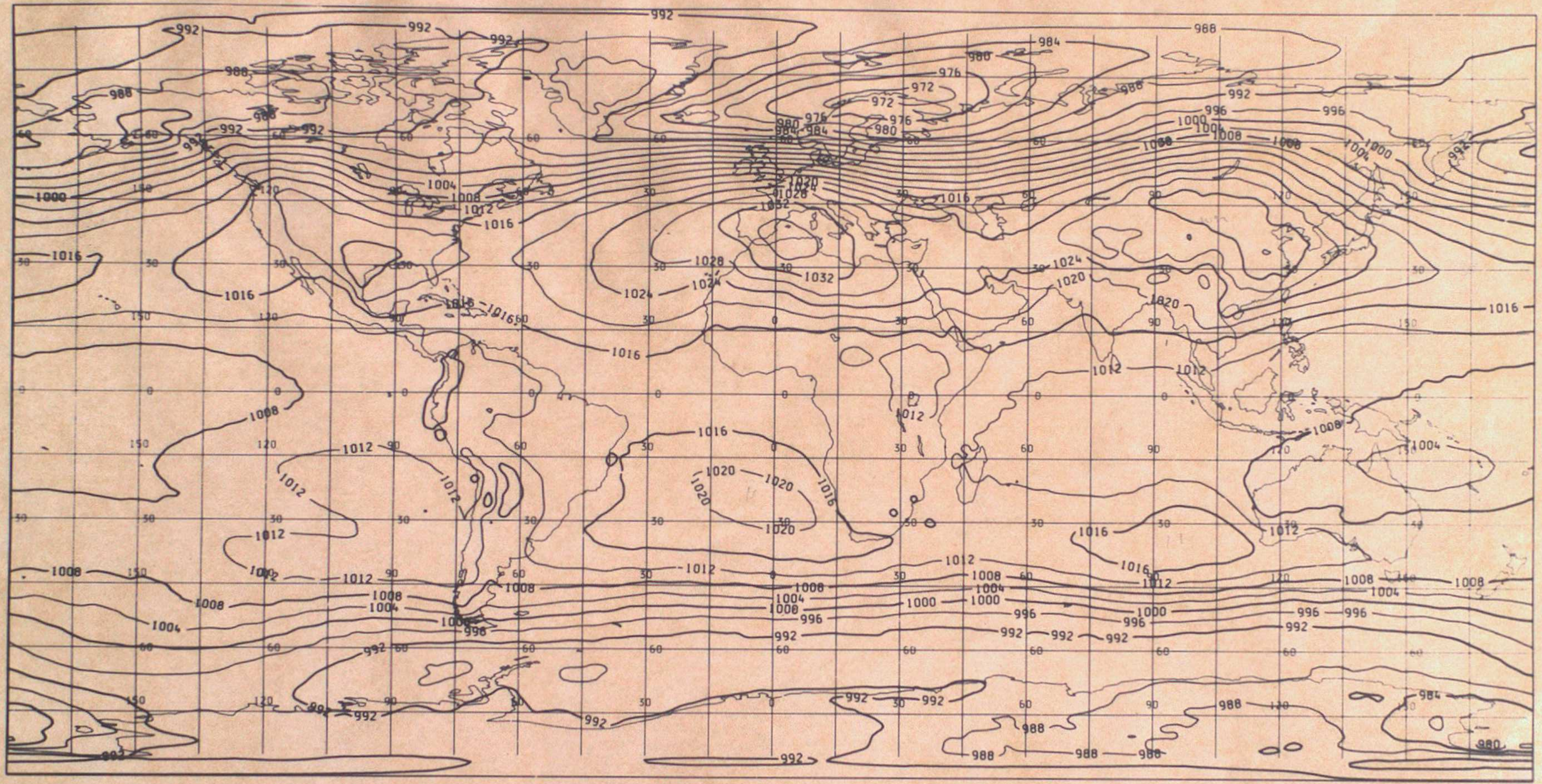

Figure 5

DC8E1342 MSL PRESSURE (MB)
ISOBARS EVERY 4MB
AVERAGE FROM 0Z ON DAY 13 TO 0Z ON DAY 42
LEVEL: SEA LEVEL EXPERIMENT NO.: 1000

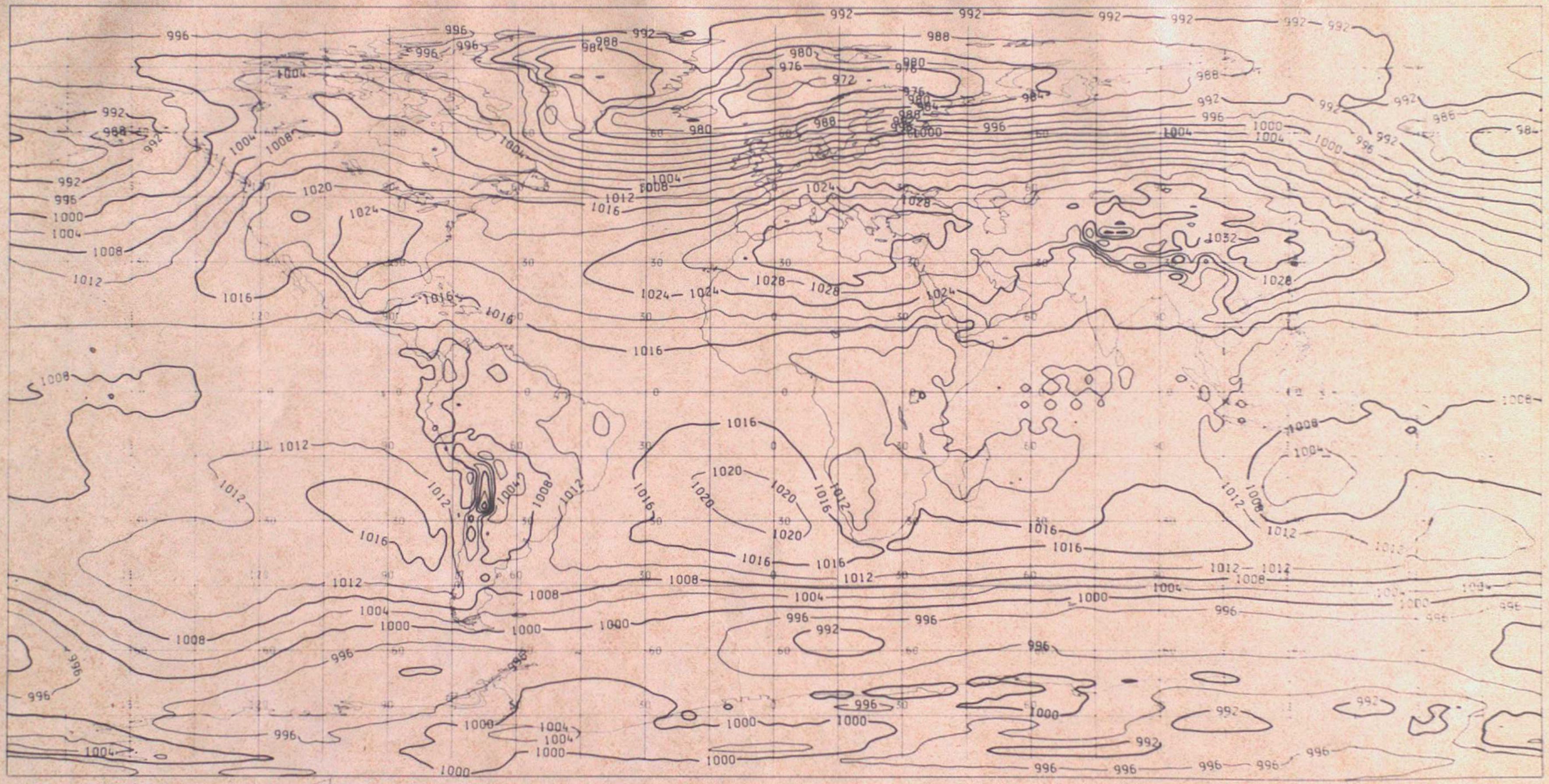

Fig 6

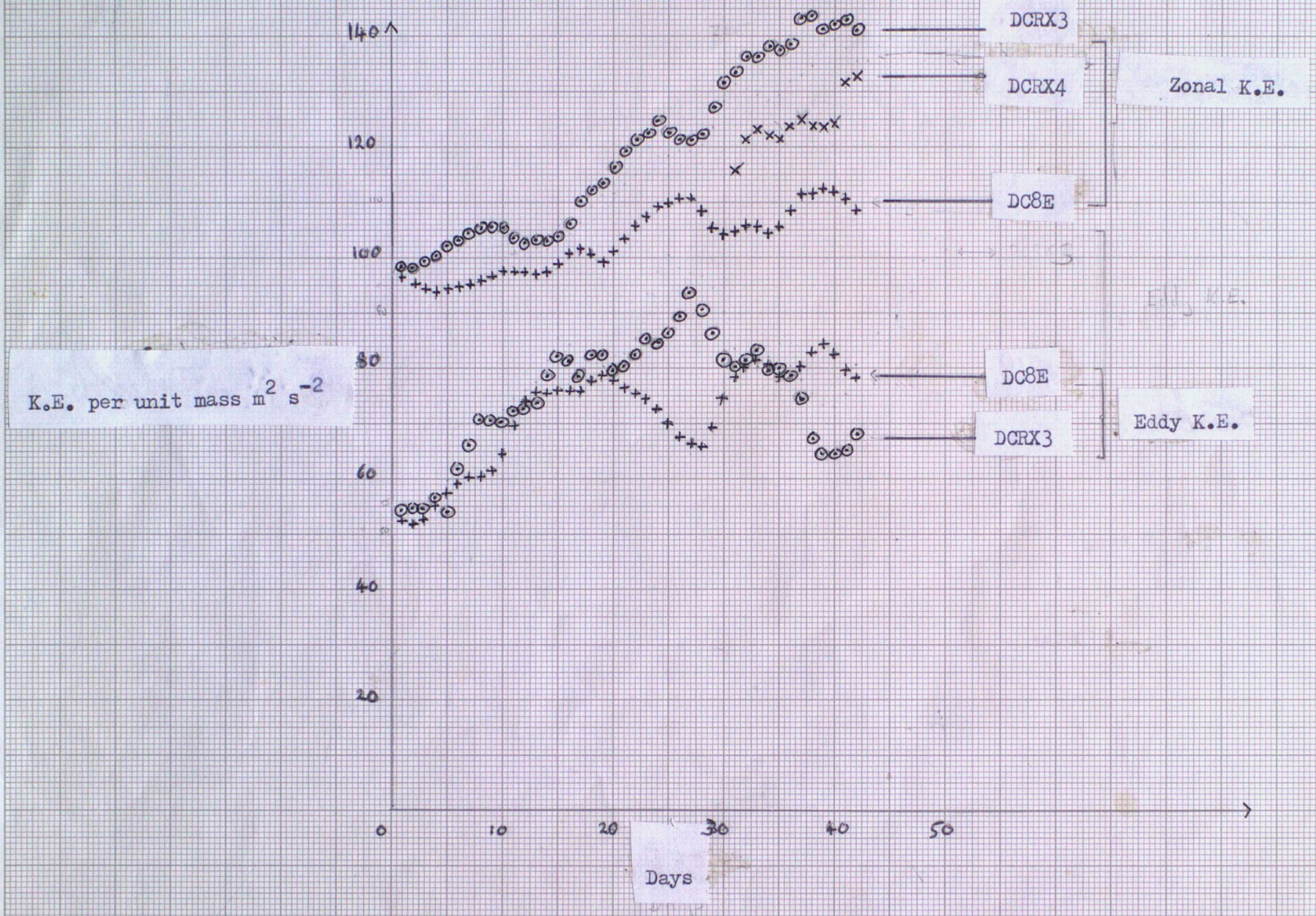


Figure 6 Global mean kinetic energies for DC8E & DCRX3

Figure 7a

DC8E1342
WESTERLY WIND
AVERAGE FROM 0Z ON DAY 13 TO 0Z ON DAY 42
ZONAL AVERAGE EXPERIMENT NO.: 1000

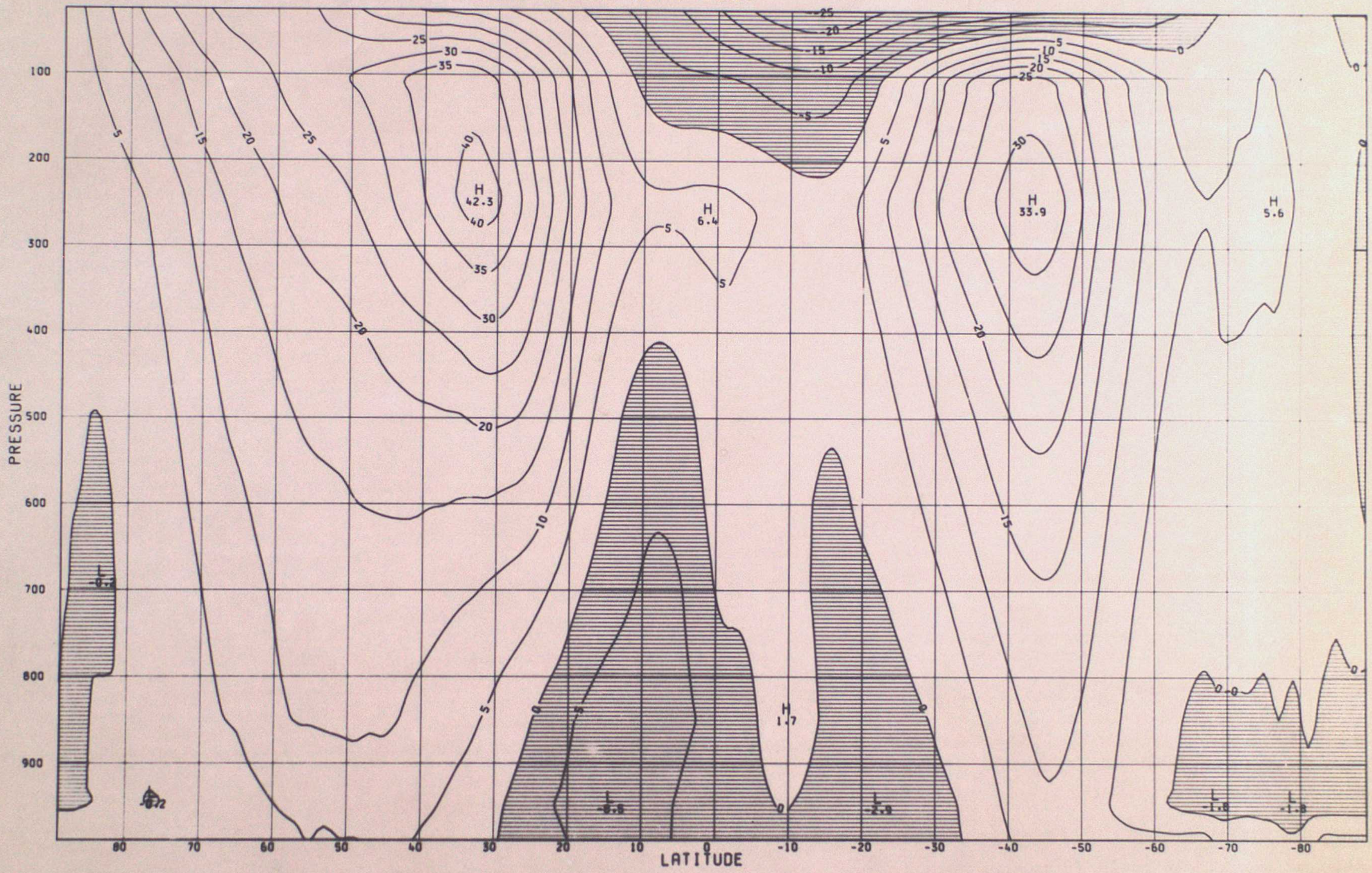

Figure 7b

DCRX3M13
WESTERLY WIND
VALID AT 0Z ON 13/0
ZONAL AVERAGE

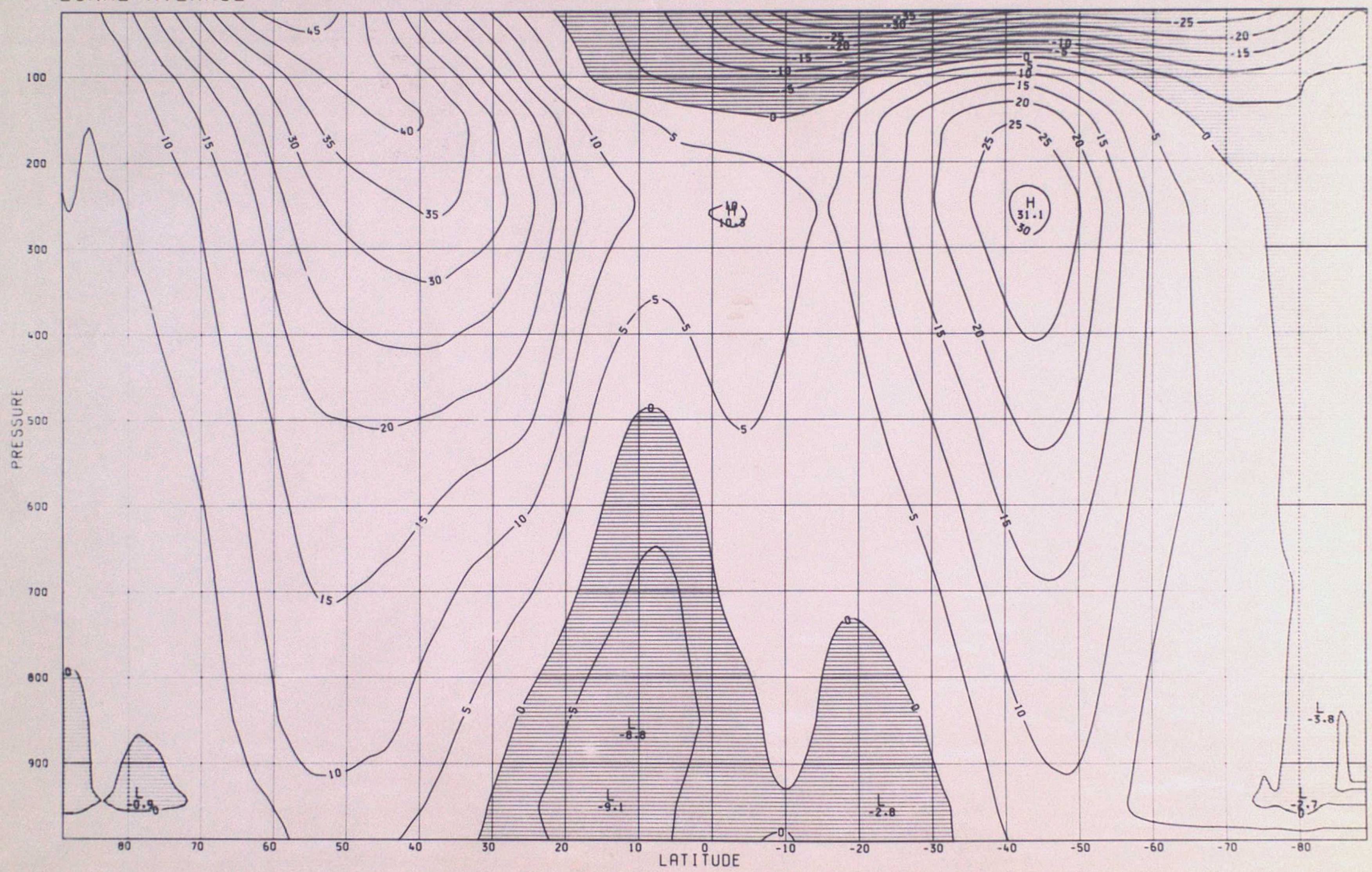

Figure 7c

FGGE EXPERIMENTS: M20.EC3BMNVR.JAN.U
WESTERLY WIND
AVERAGE FROM 0Z ON 5/1/79 DAY 5 TO 12Z ON 31/1/79 DAY 31
ZONAL AVERAGE

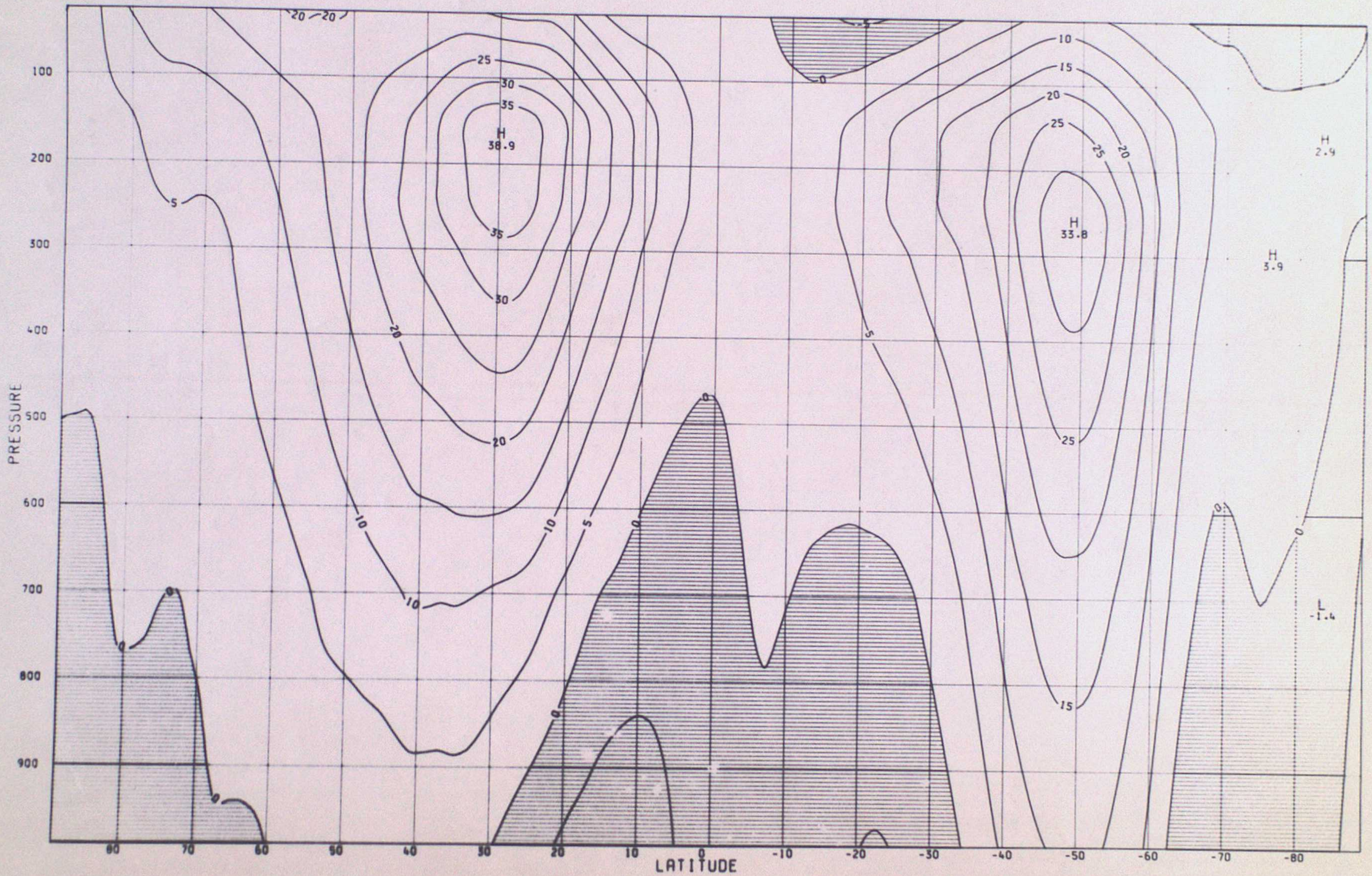

Figure 7d

DC8E1342-DCRX3M13
WESTERLY WIND
VALID AT 0Z ON 13/0
ZONAL AVERAGE

DIFFERENCES.

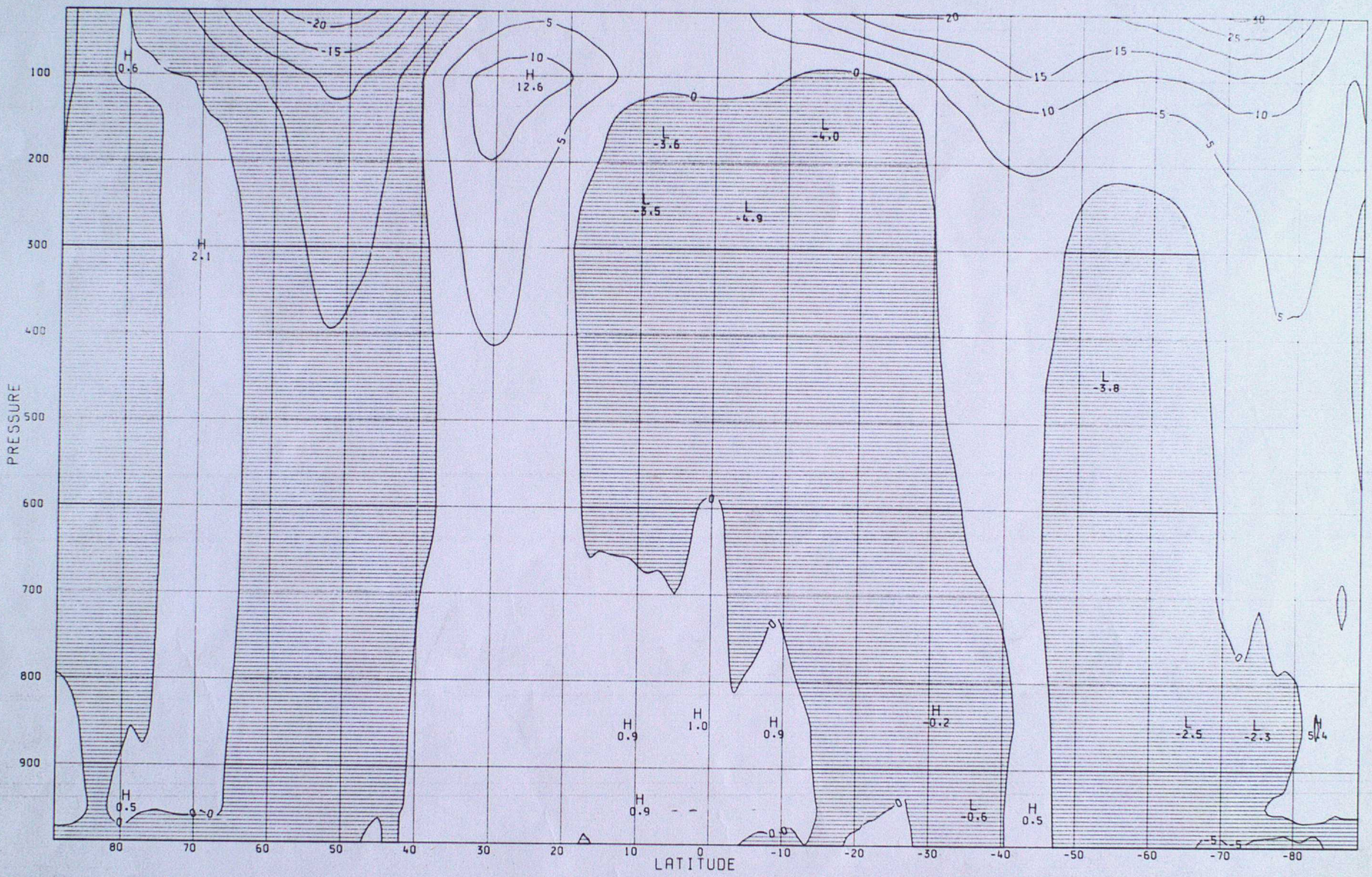

Figure 8a

DC8E1342
TEMPERATURE
AVERAGE FROM 0Z ON DAY 13 TO 0Z ON DAY 42
ZONAL AVERAGE EXPERIMENT NO.: 1000

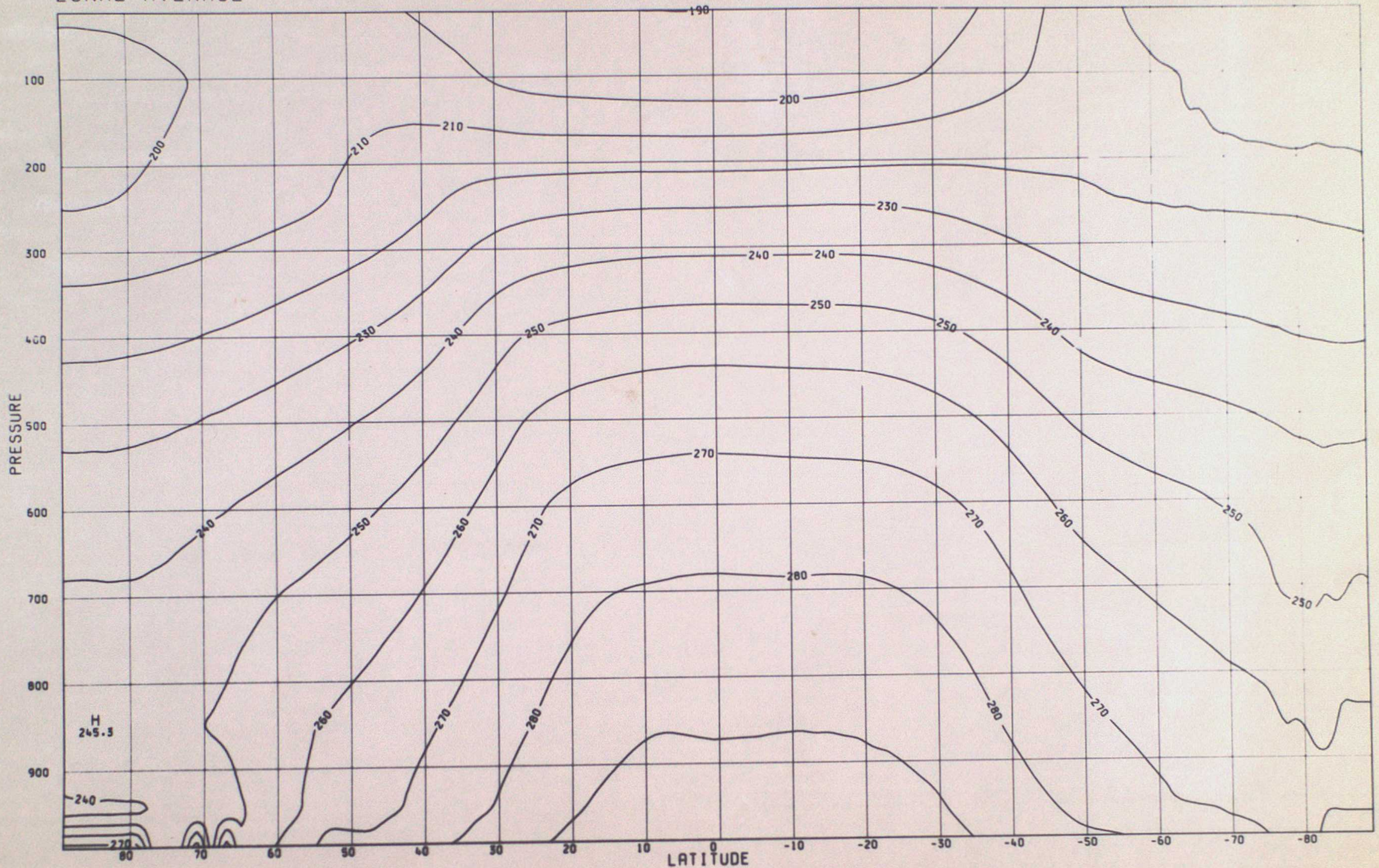

Figure 8b

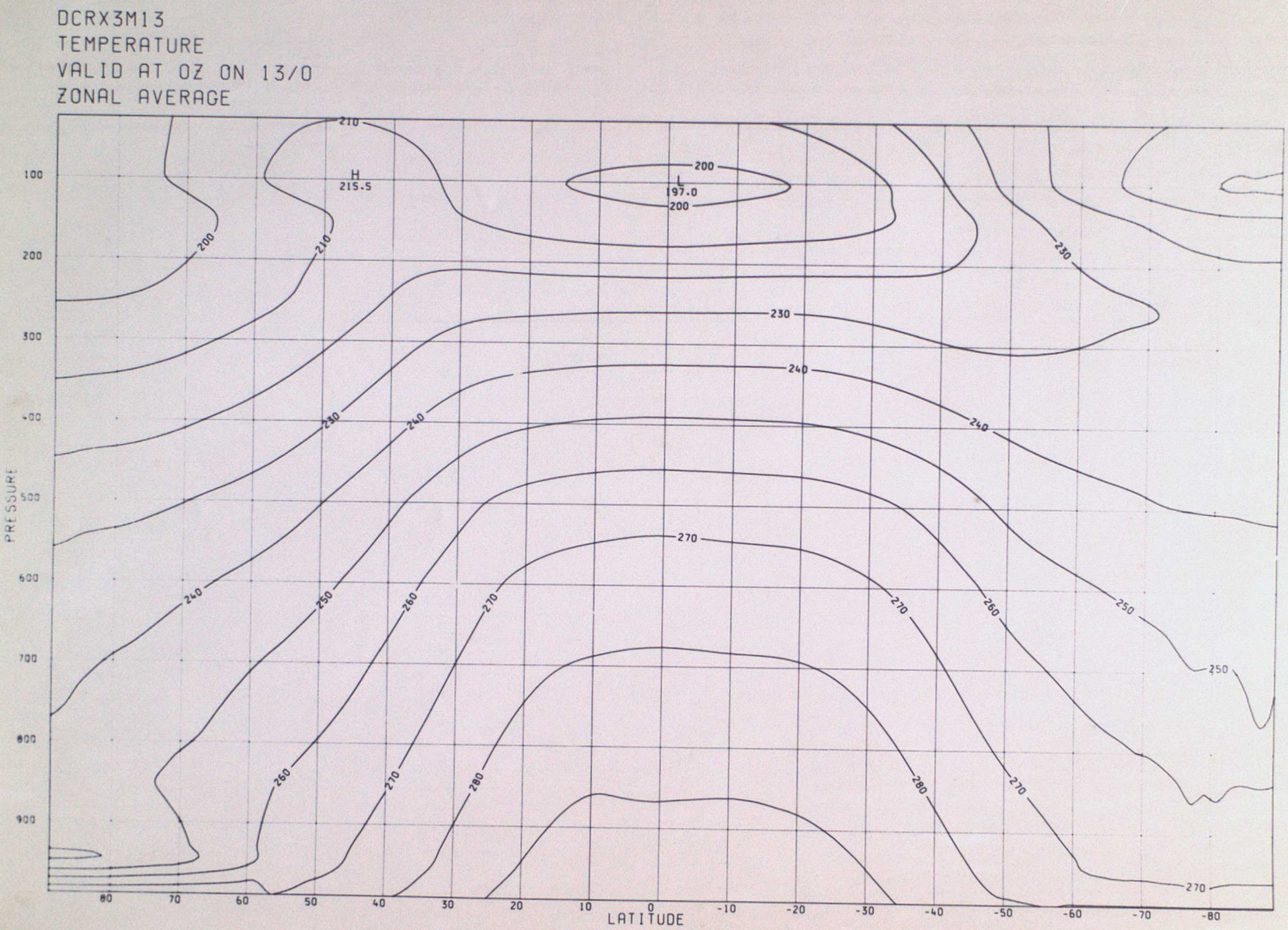
DCRX3M13
TEMPERATURE
VALID AT 0Z ON 13/0
ZONAL AVERAGE
PRESSURE
100
200
300
400
500
600
700
800
900
LATITUDE
80
70
60
50
40
30
20
10
0
-10
-20
-30
-40
-50
-60
-70
-80
H
215.5
L
197.0
200
210
230
240
250
260
270
280

Figure 8c

FGGE DATA: EC3B ANALYSIS FOR JAN
TEMPERATURE
AVERAGE FROM 0Z ON 5/1/79 DAY 5 TO 12Z ON 31/1/79 DAY 31
ZONAL AVERAGE

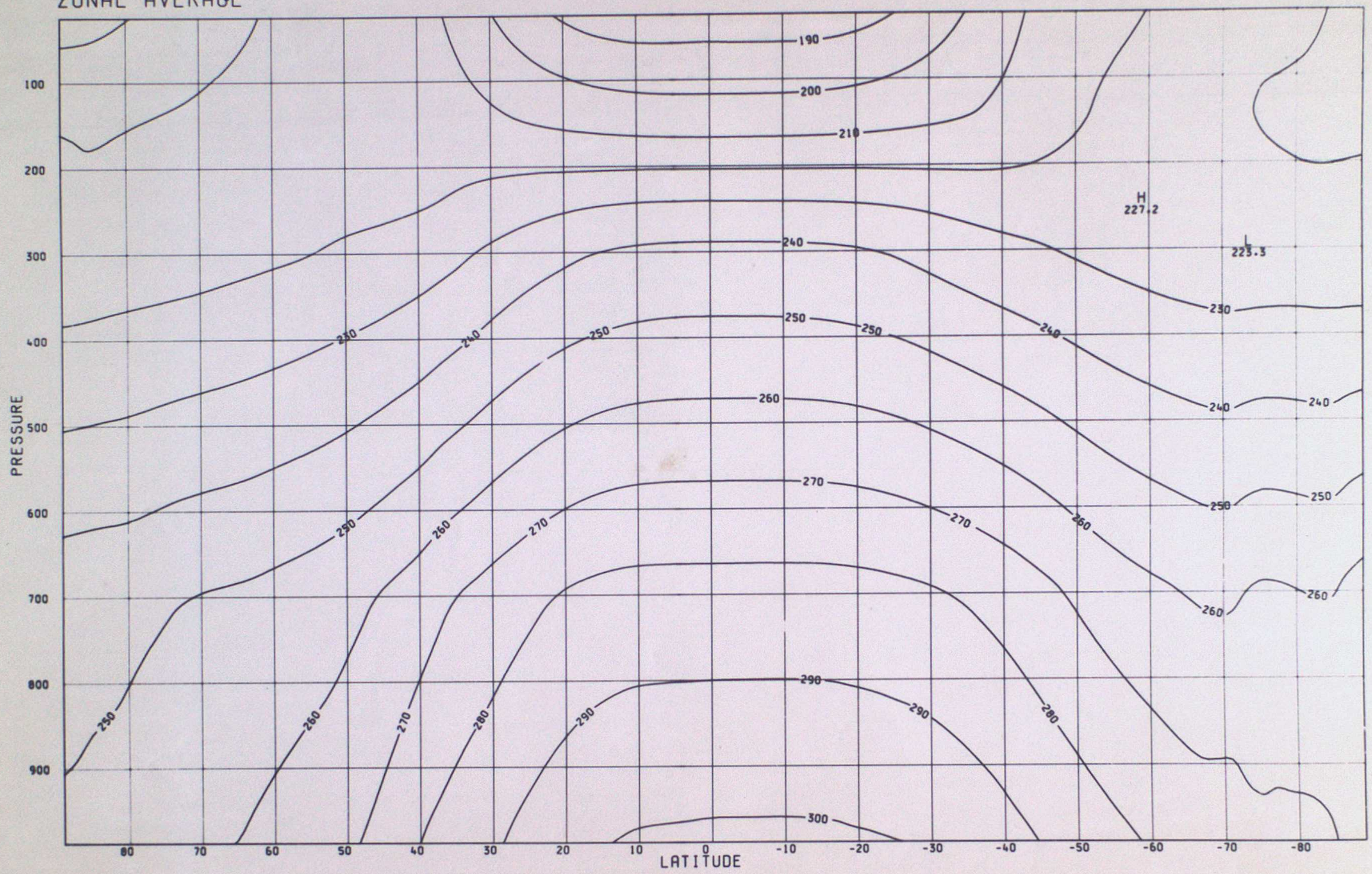

Figure 8d

DC8E1342 - DCRX3M13
TEMPERATURE
VALID AT 0Z ON 13/0
ZONAL AVERAGE

DIFFERENCES

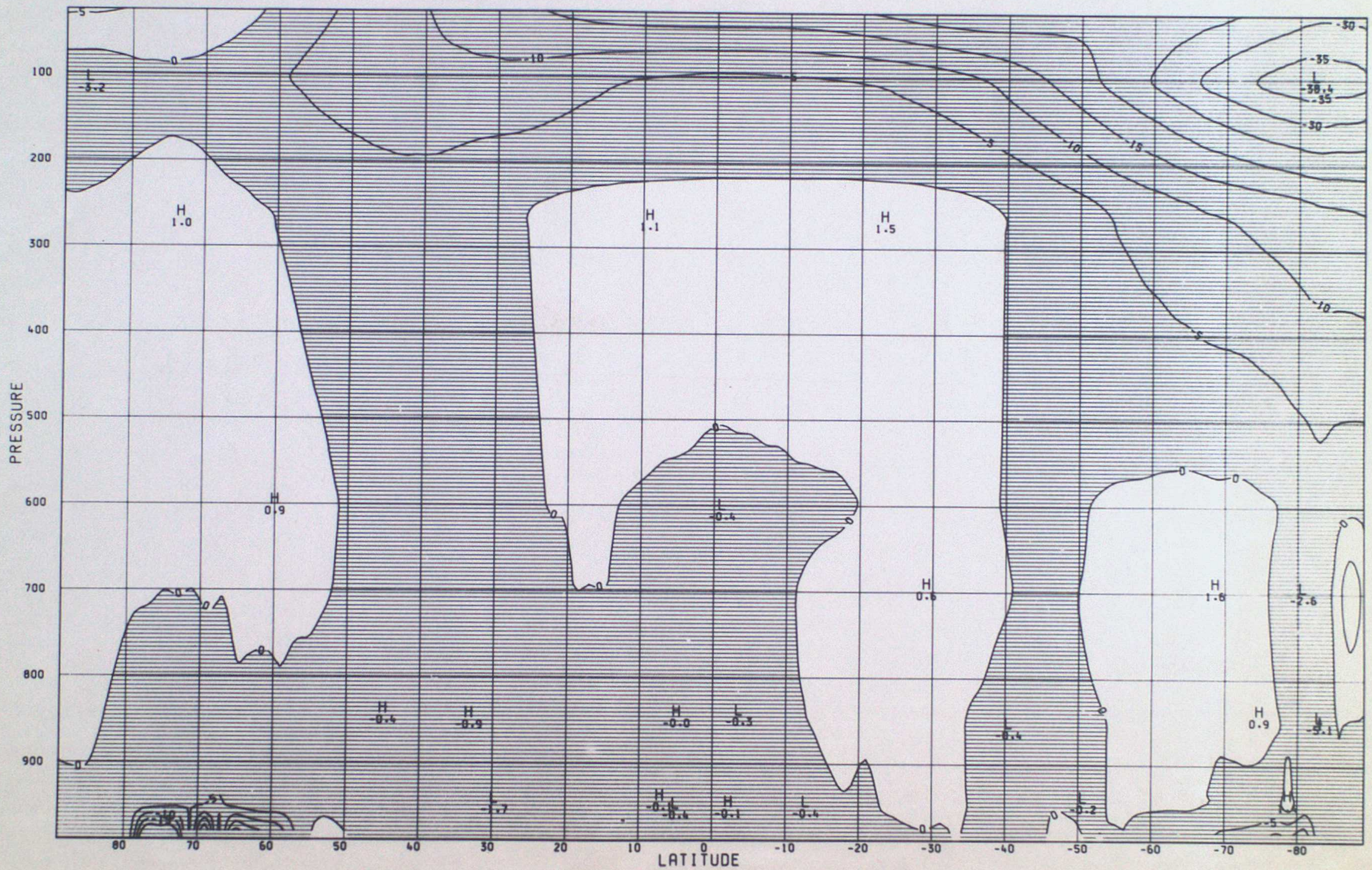

Figure 9a

DC8E1342 SURFACE TEMPERATURE (DEG K)
ISOTHERMS EVERY 5 DEG UP TO 283 THEN EVERY 2.5
AVERAGE FROM 0Z ON DAY 13 TO 0Z ON DAY 42
LEVEL: SURFACE EXPERIMENT NO.: 1000

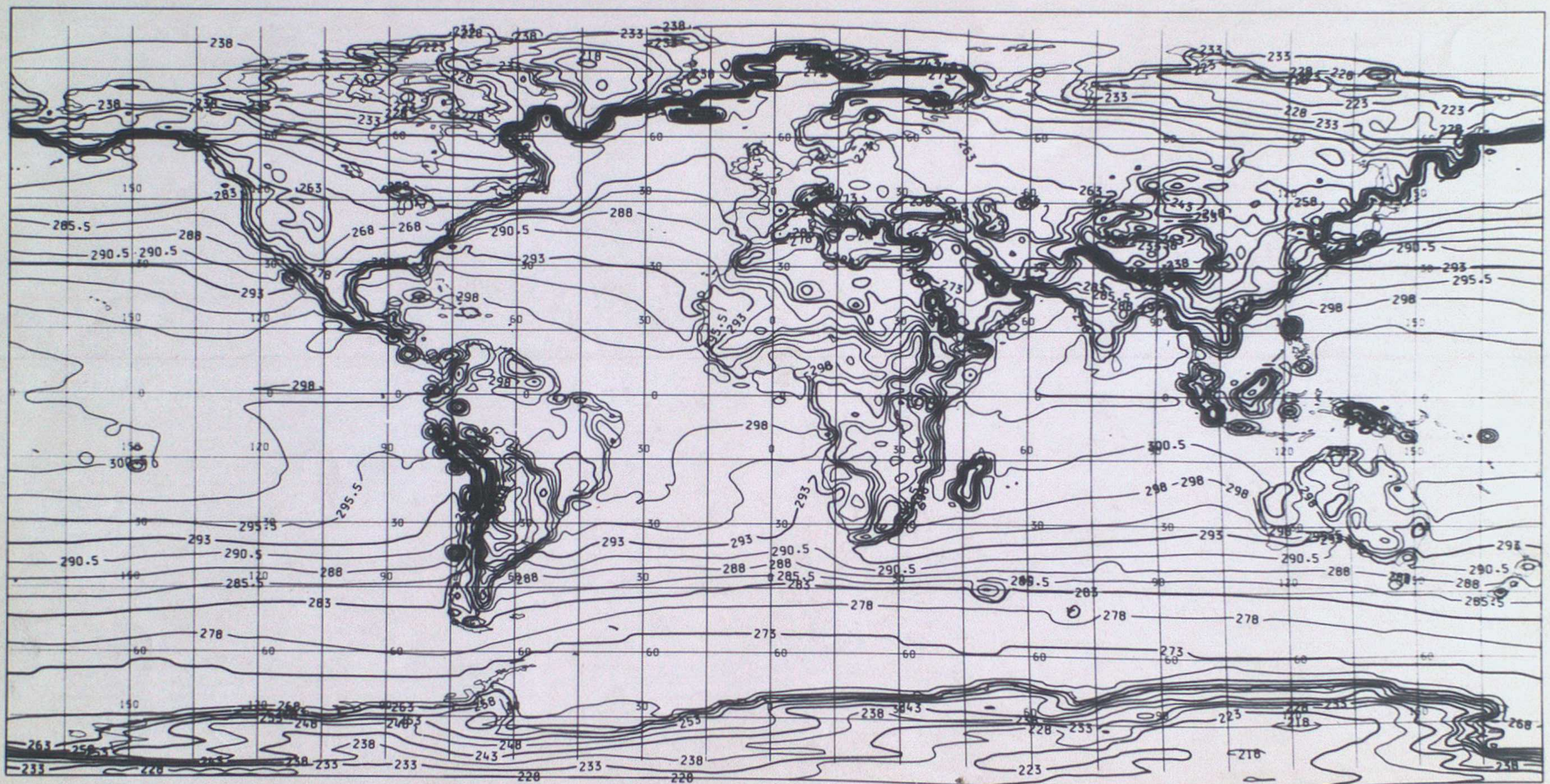

Figure 9b

DCRX3M13 SURFACE TEMPERATURE
ISOTHERMS AT INTERVALS OF 5 DEG K UP TO 283 DEG THEN EVERY 2.5 DEG
VALID AT OZ ON 13/0
LEVEL: SURFACE

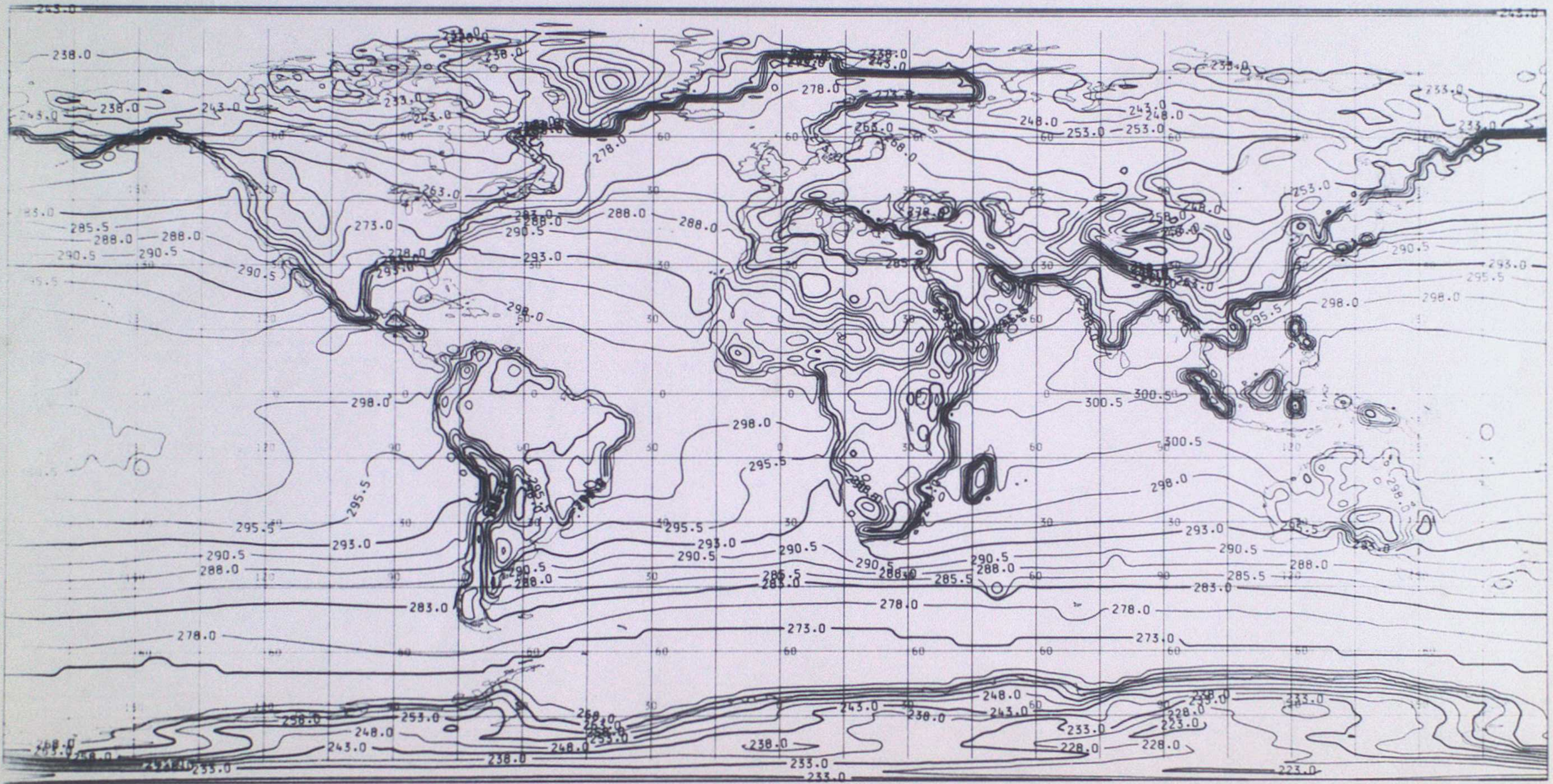

Figure 9c

DCRX3M13 DIFFERENCE IN TEMPERATURE AT SURFACE
-DC8E1342 ISOPLETHS AT UNIT INTERVALS. UNITS: DEG K
VALID AT 0Z ON 13/0
LEVEL: SURFACE

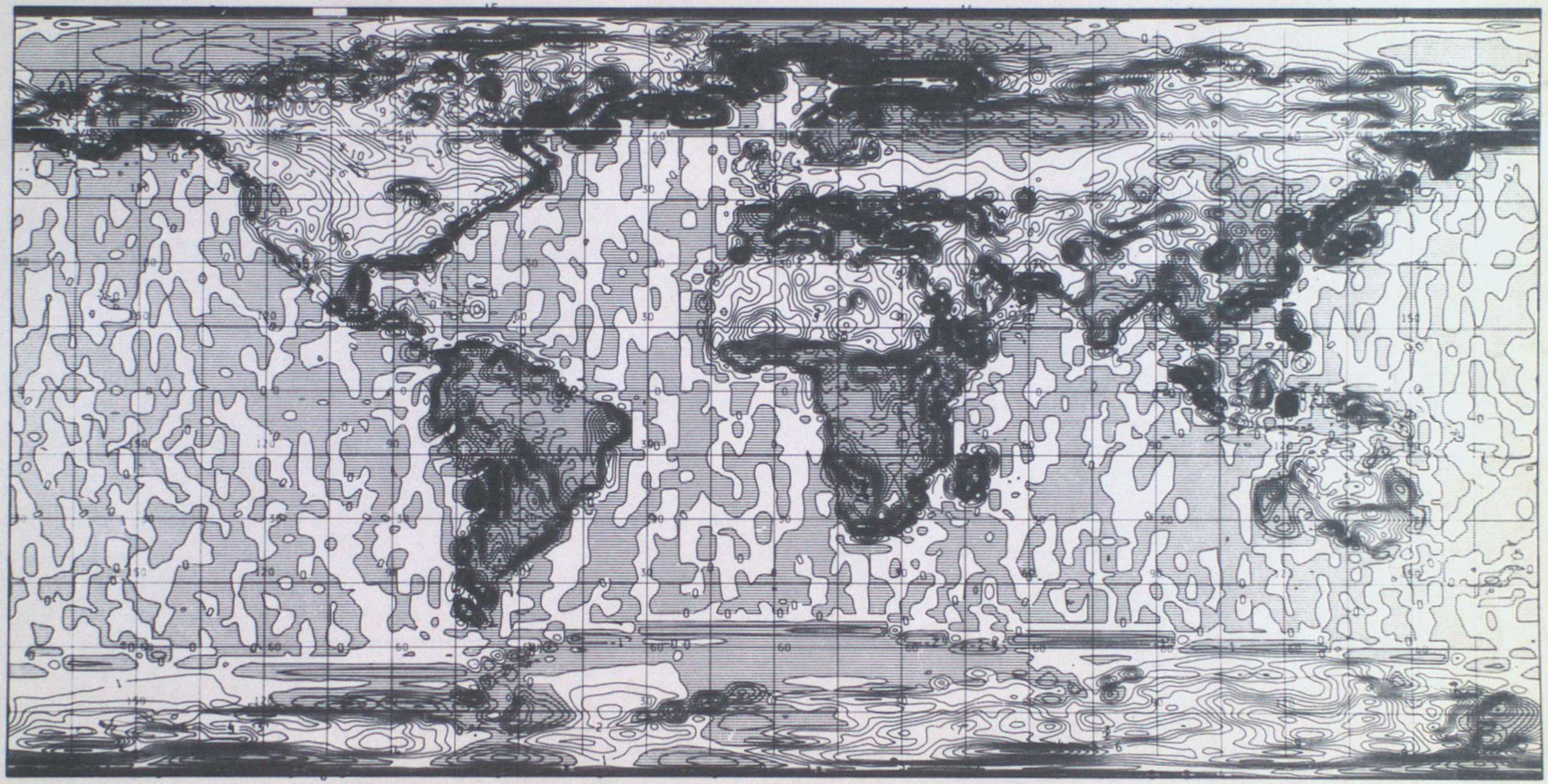

Figure 10a

DC8E1342 SOIL MOISTURE CONTENT
ISOPLETHS AT 0.3, 1.25, 2.5, 5, 10 AND 14.5 CM. SHADED BELOW 5 CM
FROM 0Z ON DAY 13 TO 0Z ON DAY 42
LEVEL: SURFACE EXPERIMENT NO.: 1000

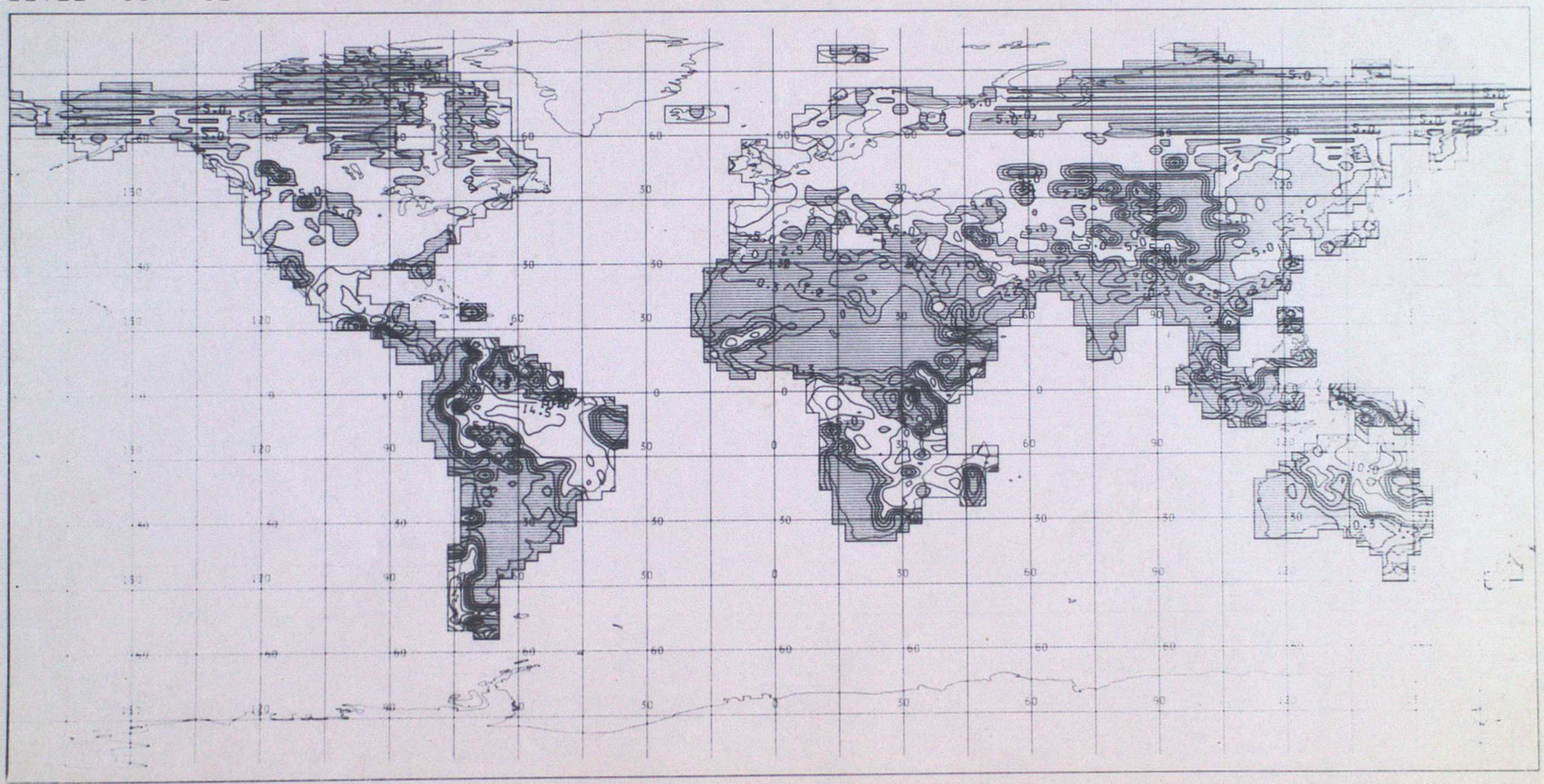

Figure 10b

DCRX3M13 SOIL MOISTURE CONTENT
ISOPLETHS AT 0.3, 1.25, 2.5, 5, 10 AND 14.5 CM. SHADED BELOW 5 CM
VALID AT 0Z ON 13/0
LEVEL: SURFACE

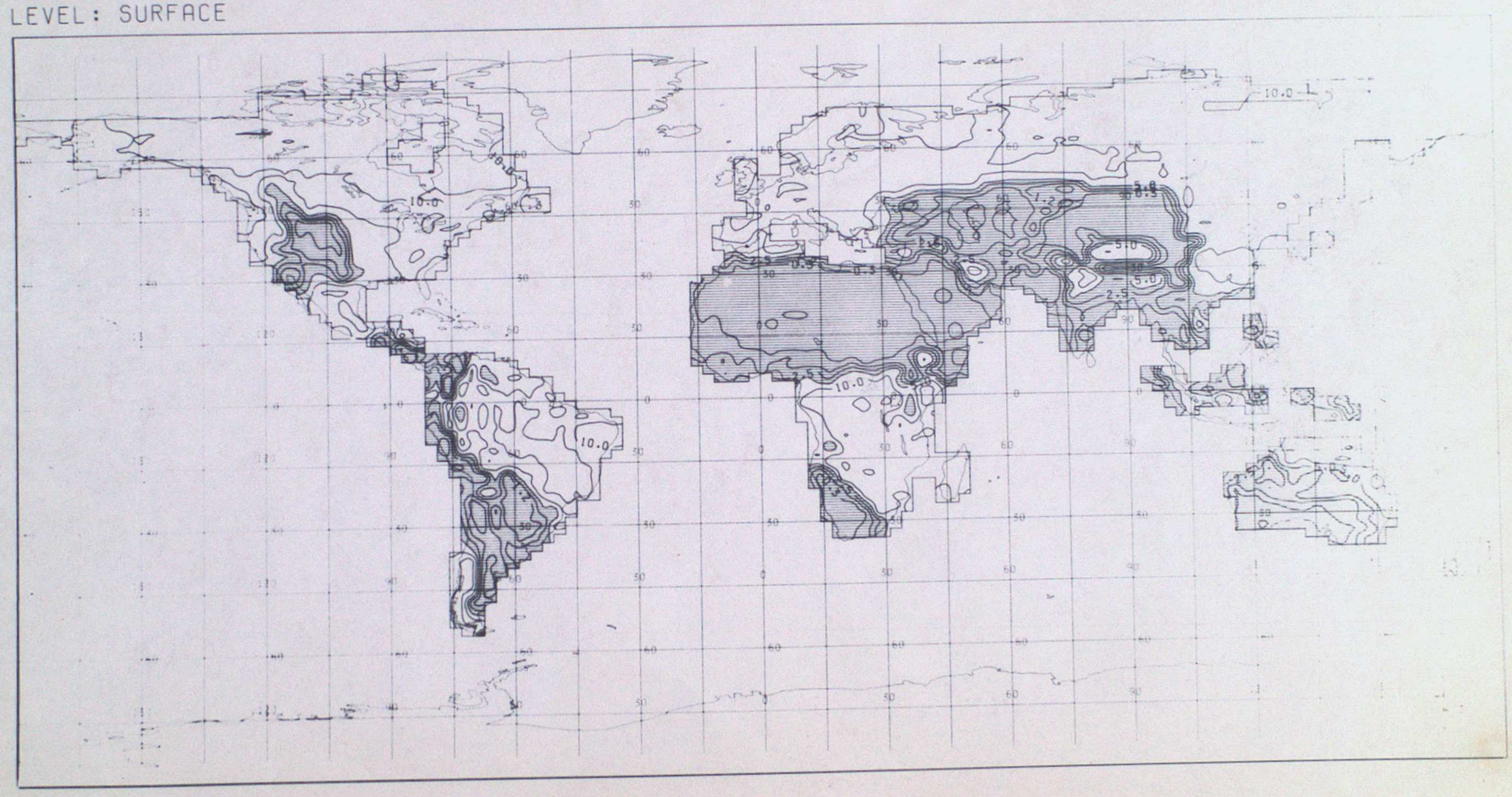

DCRX3M13 DIFFERENCE IN SOIL MOISTURE CONTENT
-DC8E1342 ISOPLETHS AT 0.0 AND +/- 1, 2 AND 5 CM. SHADED NEGATIVE
VALID AT 0Z ON 13/0
LEVEL: SURFACE

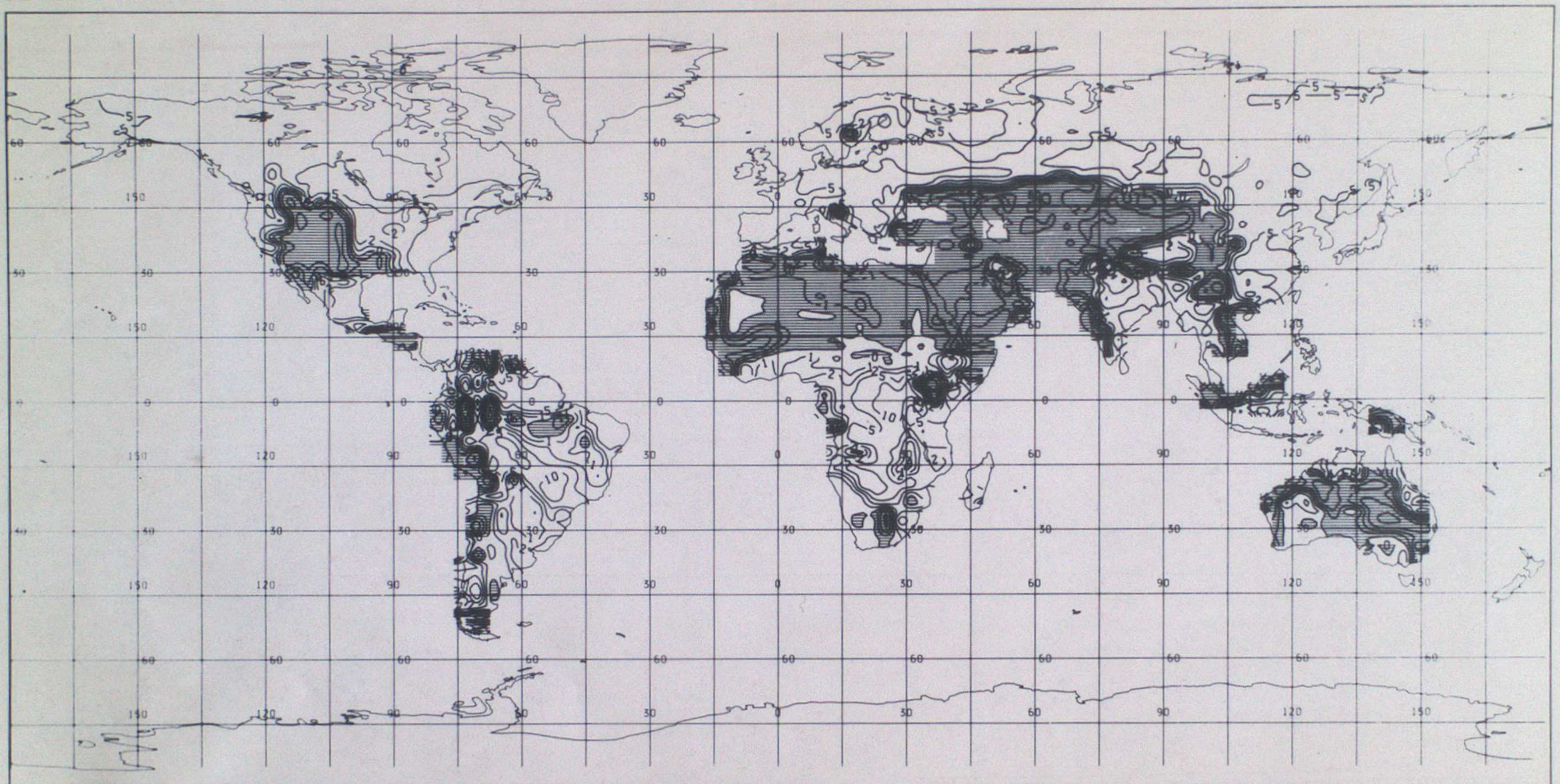

Figure 11 Zonal mean precipitation (January case)

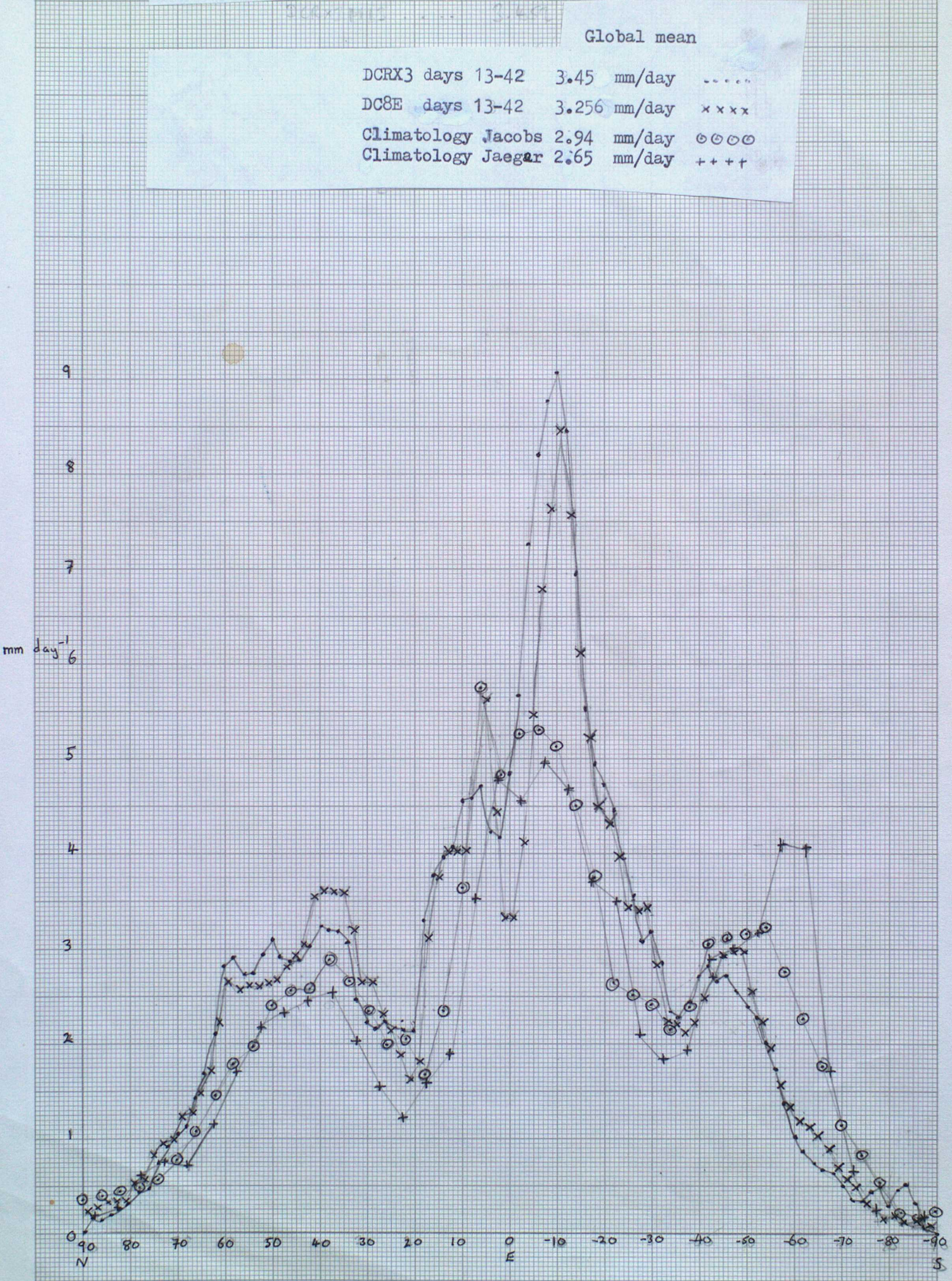

Figure 12

DC8E1342    TOTAL PRECIPITATION    (MM/DAY)
ISOPLETHS AT 1 2 5 10 THEN EVERY 20
AVERAGE FROM 0Z ON DAY 13 TO 0Z ON DAY 42
LEVEL: SURFACE    EXPERIMENT NO.: 1000

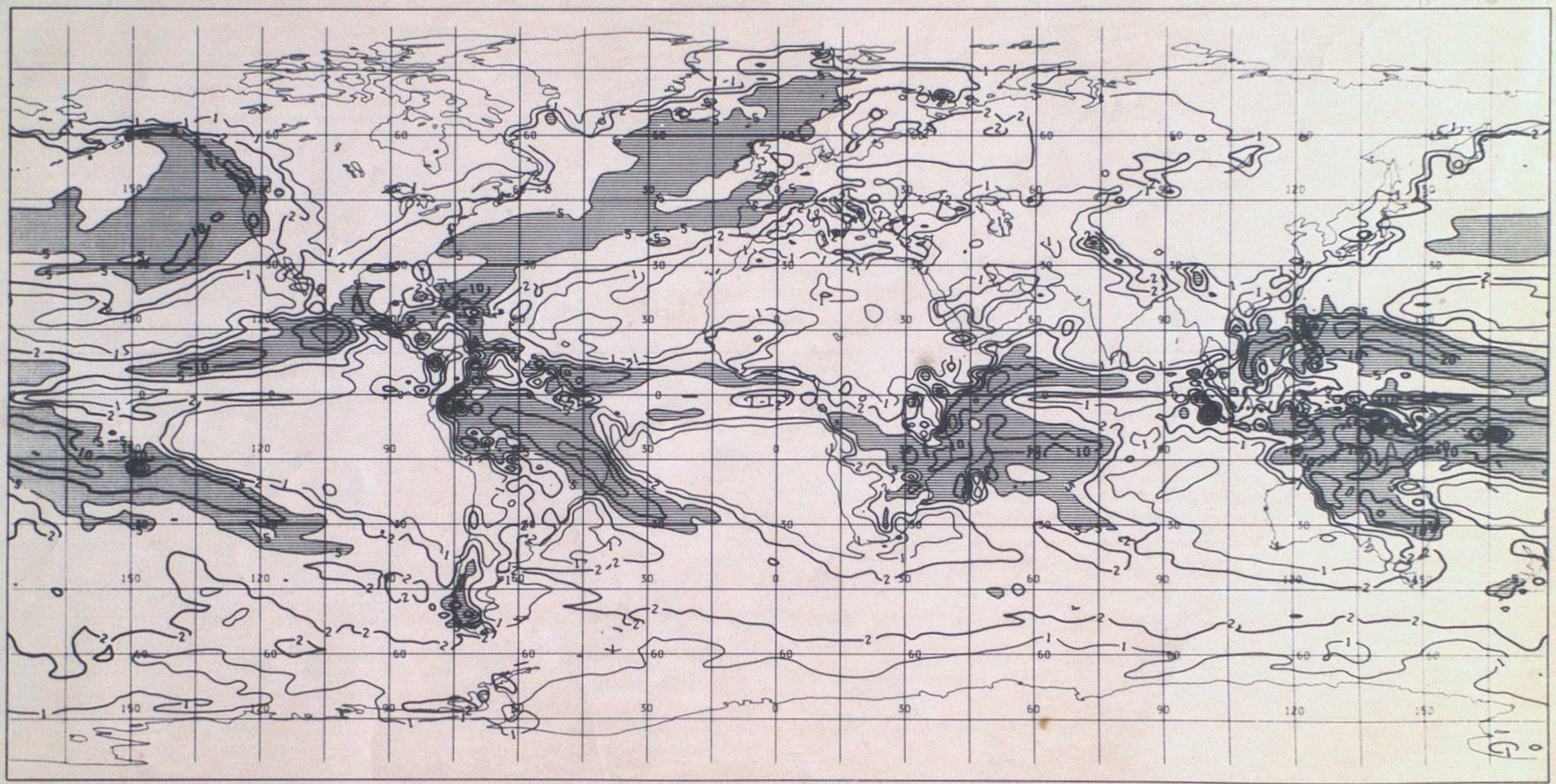

Figure 13

DCRX3M13 TOTAL PRECIPITATION (MM/DAY)
ISOPLETHS AT 1 2 5 10 THEN EVERY 20
VALID AT OZ ON 13/0
LEVEL: SURFACE

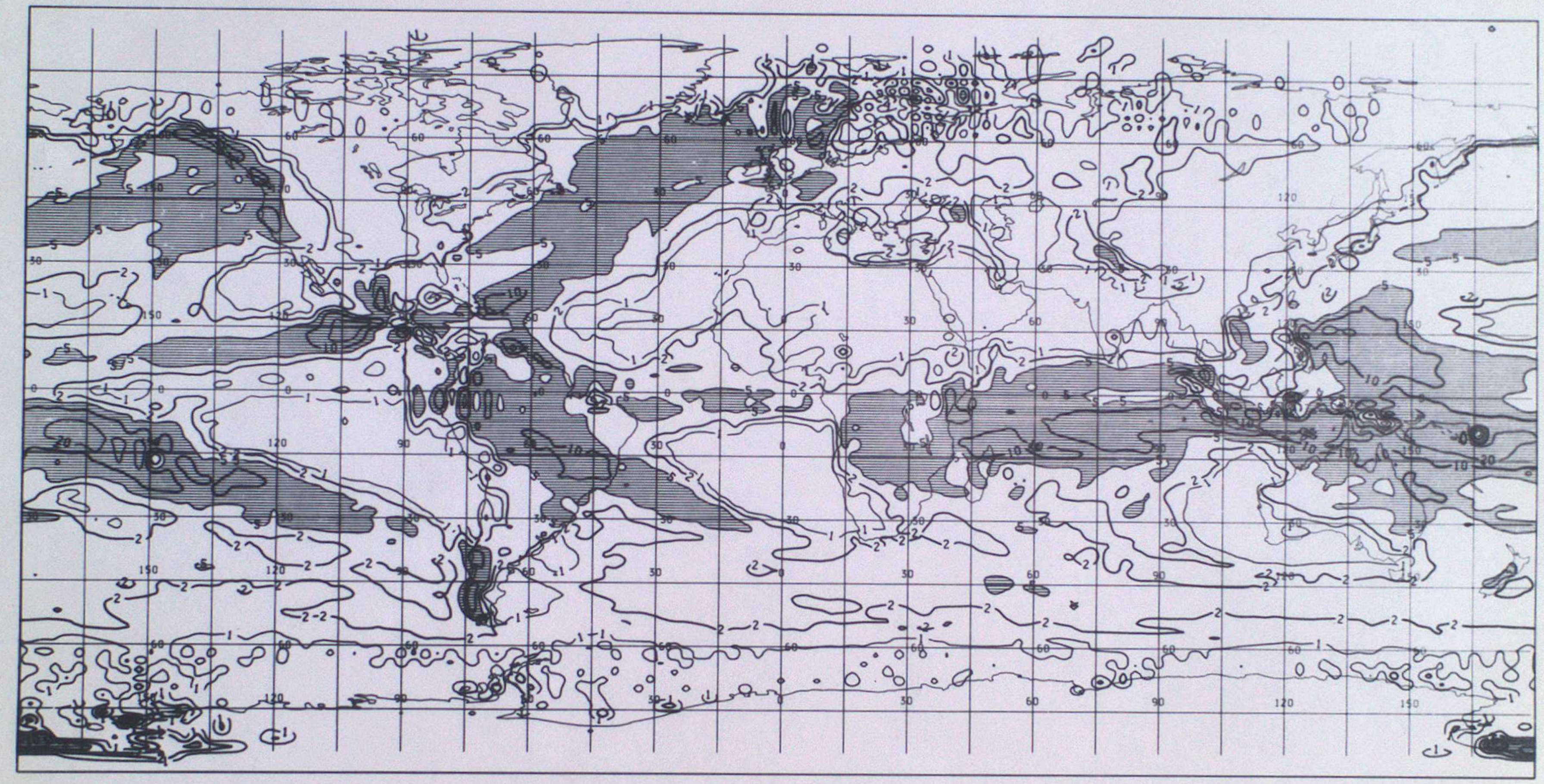

Figure 13a

DIFFERENCE MAP DCRX3M13 - DCE81342 TOTAL PRECIPITATION
ISOPLETHS AT +/- 1, 2 AND EVERY 5 MM. NEGATIVE AREAS SHADED
VALID AT 0Z ON 13/0
LEVEL: SURFACE

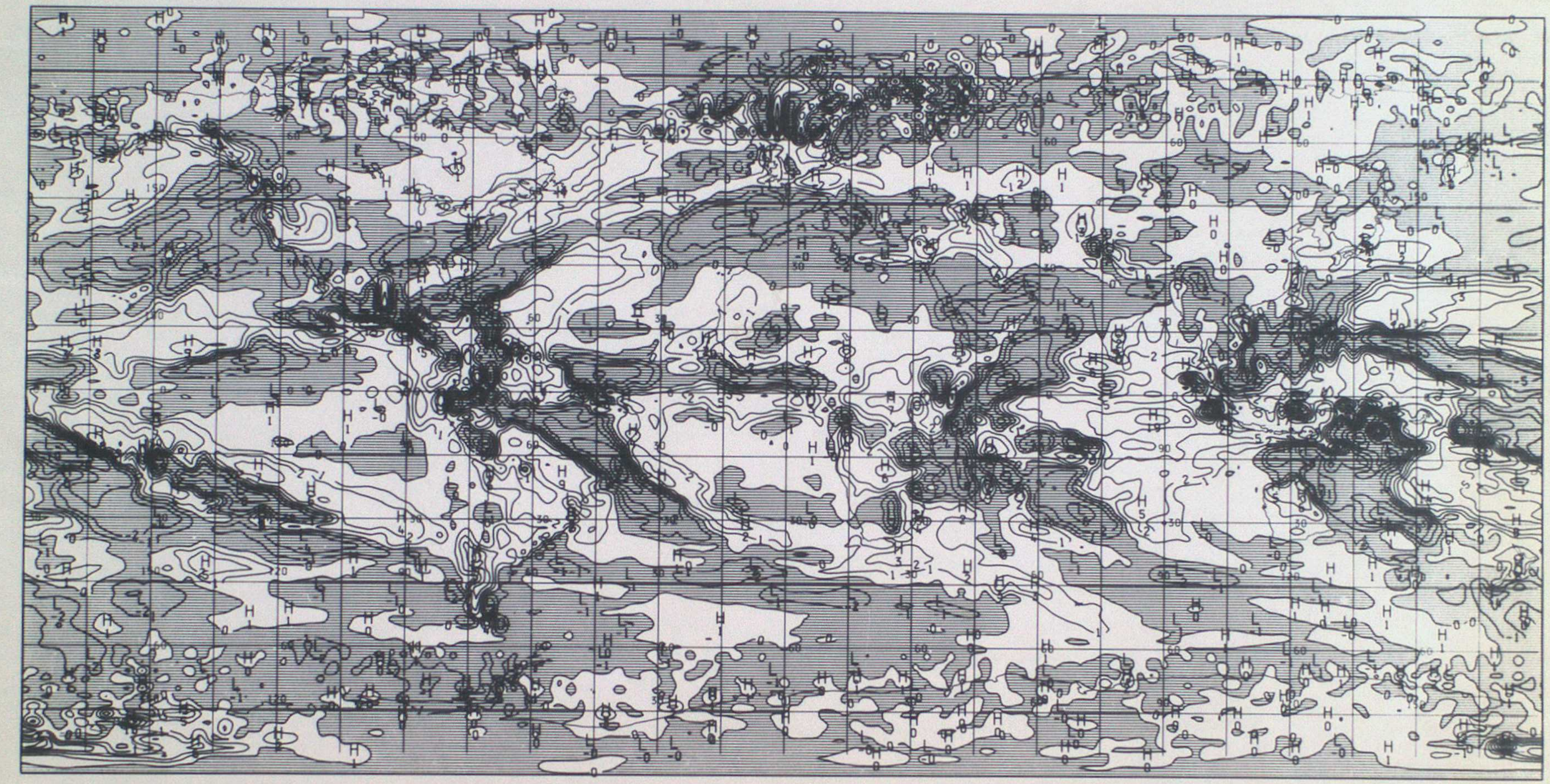

Figure 14

DJF PRECIPITATION FROM MOLLER MM/DAY
AVERAGE FROM 0Z ON 1/12 DAY 334 TO 0Z ON 28/2 DAY 59
LEVEL: SURFACE

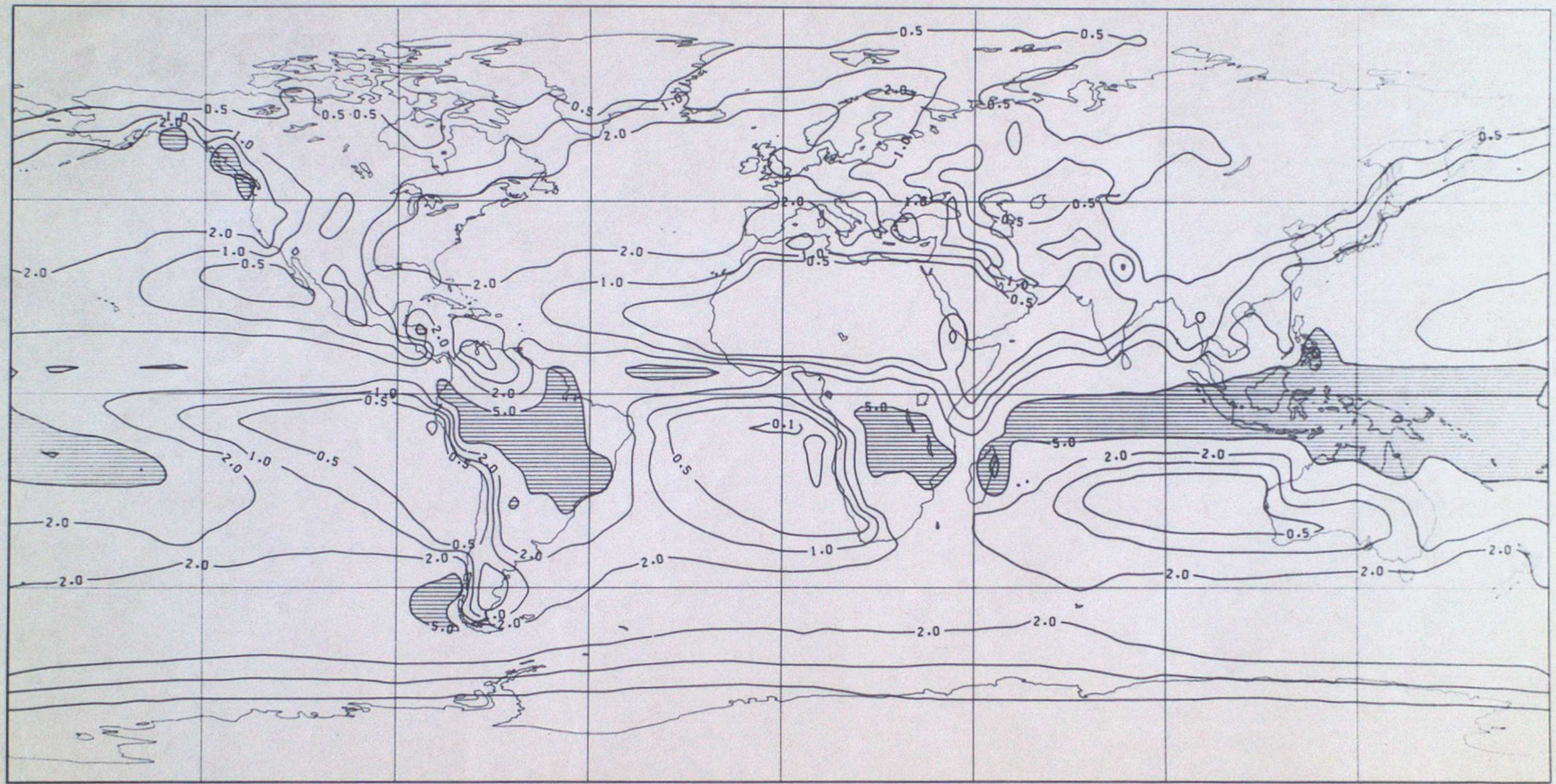

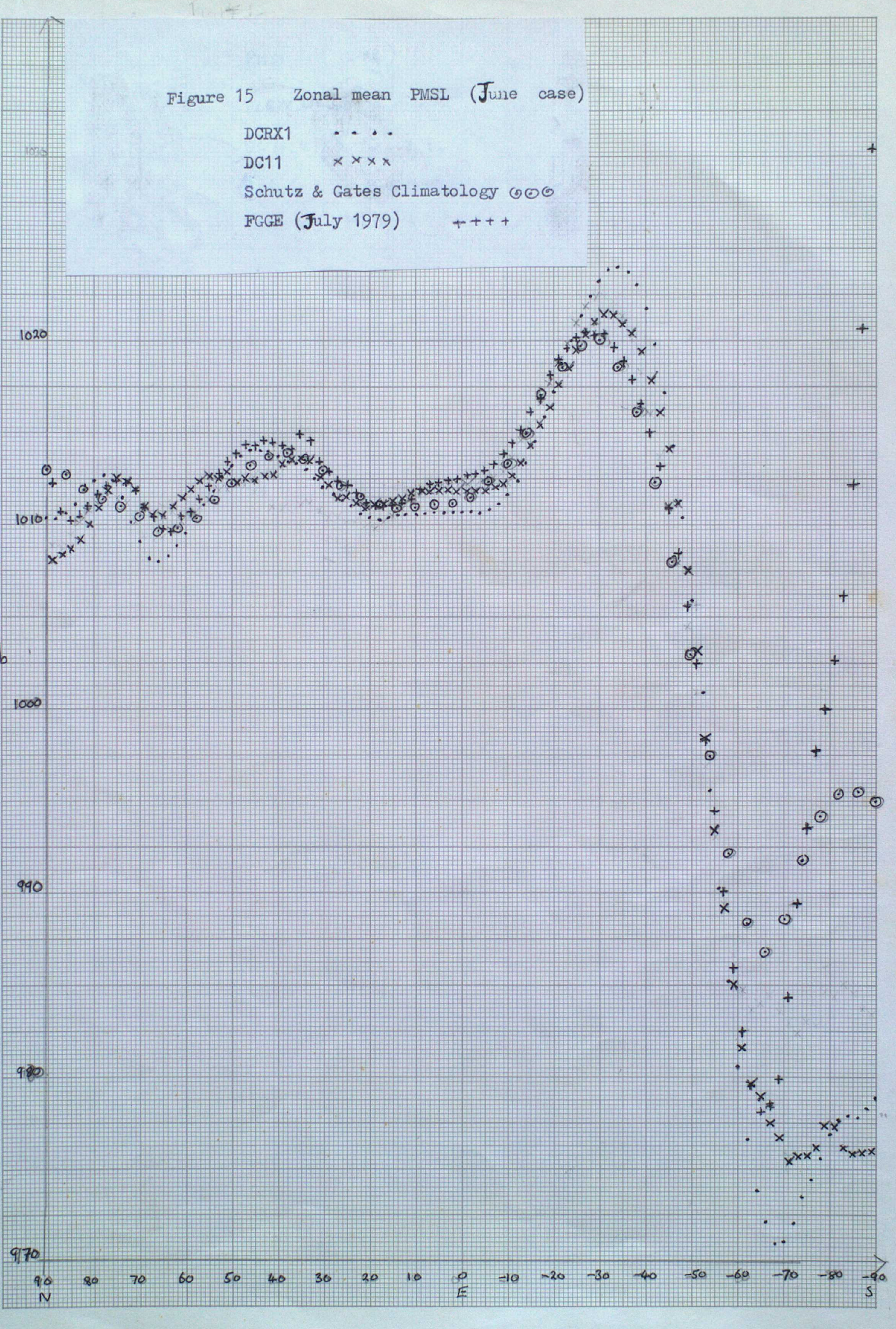
Figure 15 Zonal mean PMSL (June case)
DCRX1
DC11
Schutz & Gates Climatology
FGGE (July 1979)
1020
1010
mb
1000
990
980
970
90
N
80
70
60
50
40
30
20
10
0
E
-10
-20
-30
-40
-50
-60
-70
-80
-90
S

Figure16

DC112150 PMSL

AVERAGE FROM 0Z ON 2/12 DAY 21 TO 0Z ON 1/1/1 DAY 50
LEVEL: SEA LEVEL EXPERIMENT NO.: 1229

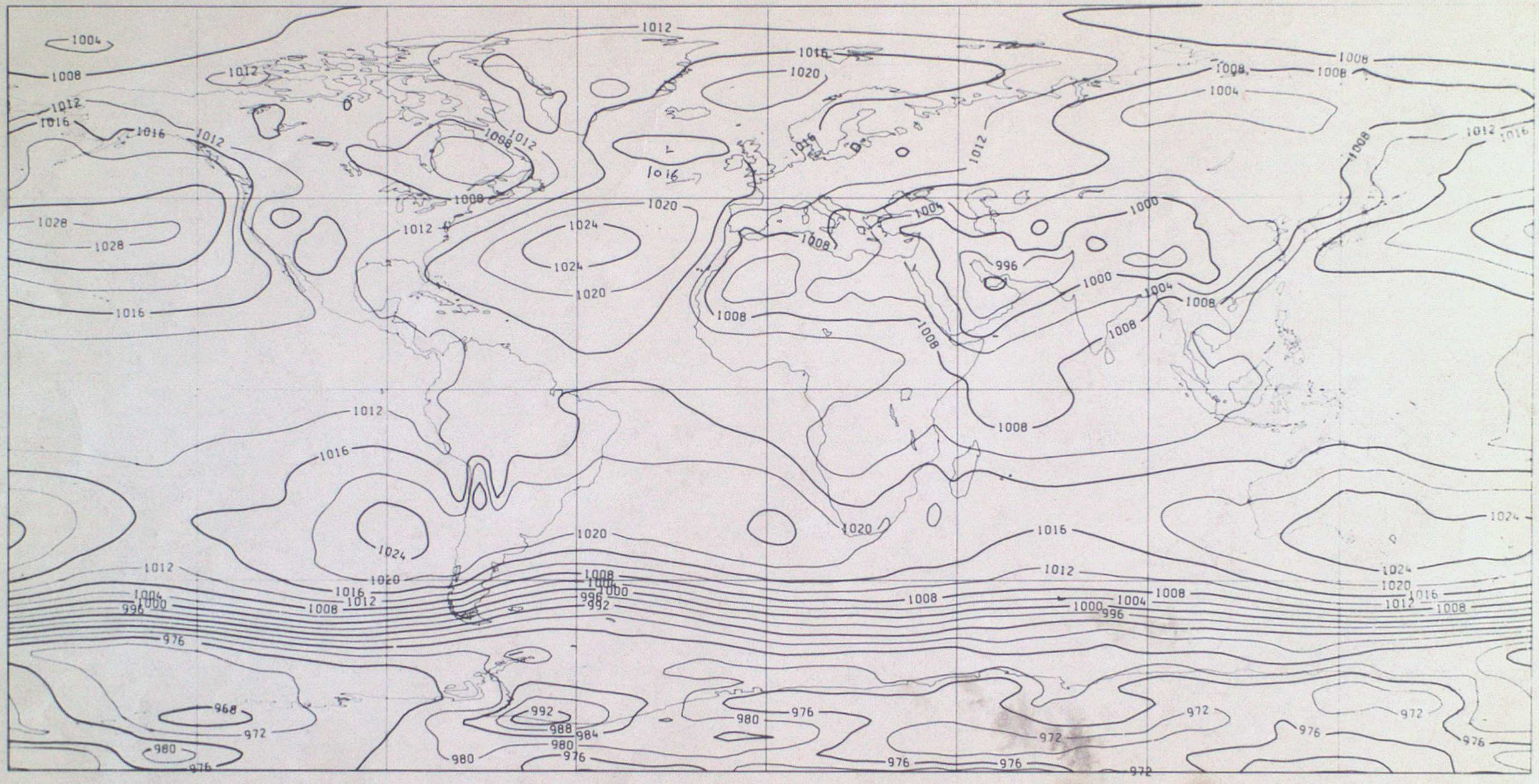

Figure 17

DCRX1M35 PMSL

VALID AT OZ ON 17/8/1982  DATA TIME OZ ON 27/7/1982
LEVEL: SEA LEVEL

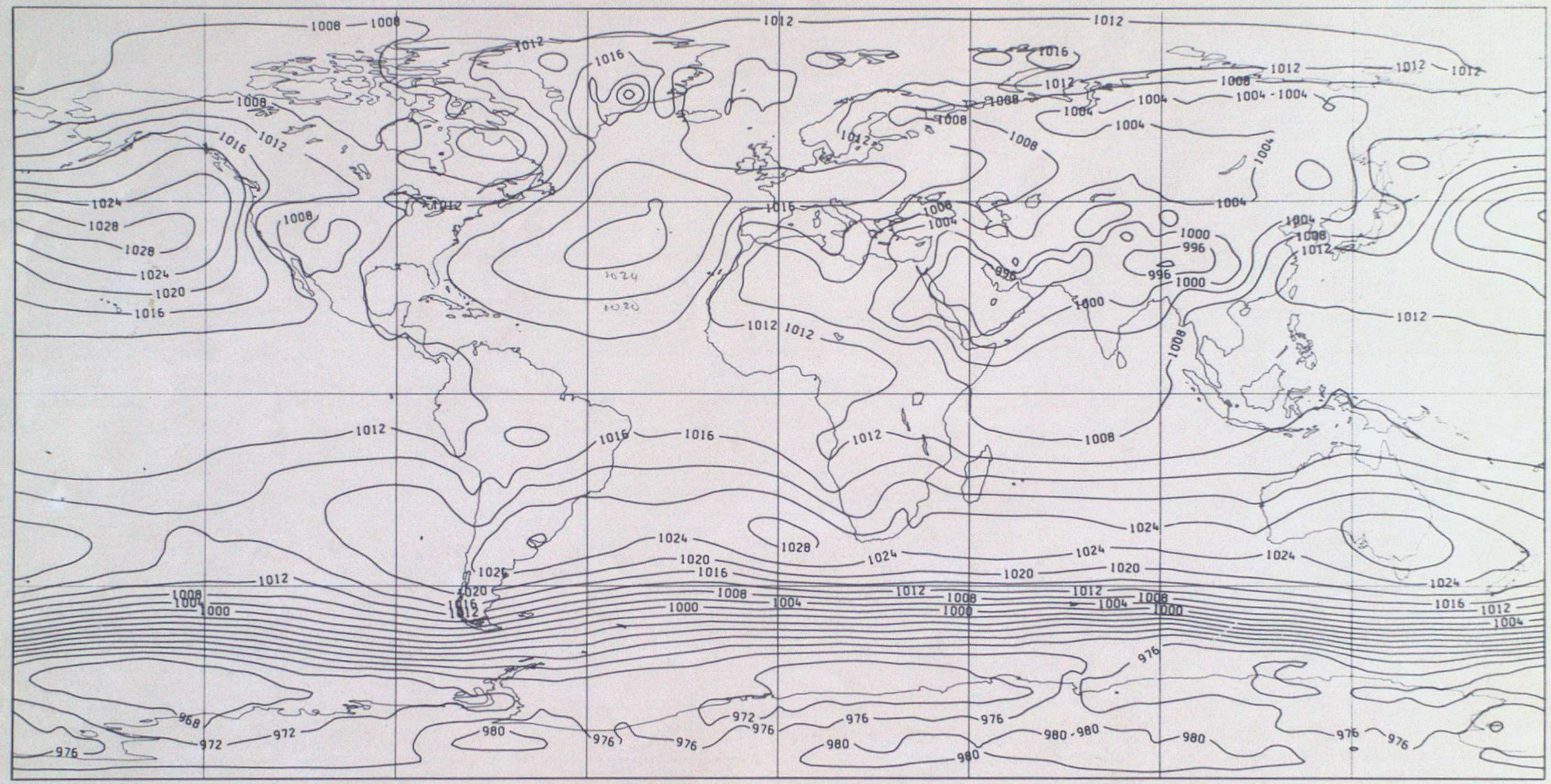

Figure 18

SCHUTZ AND GATES DATA
JULY PMSL
AVERAGE FROM OZ ON 1/7 DAY 182 TO OZ ON 31/7 DAY 212
LEVEL: SEA LEVEL

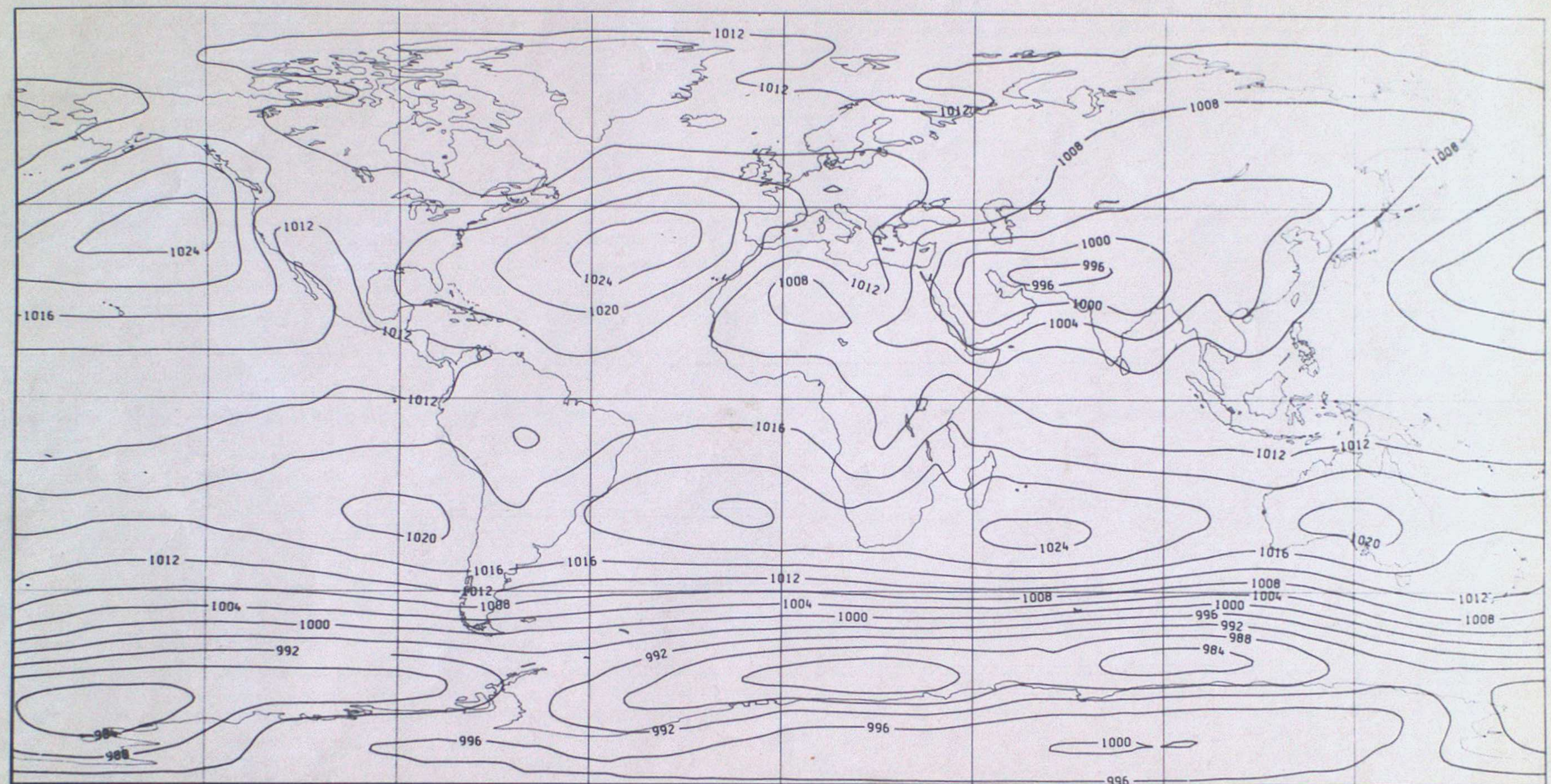

Figure 19 Time evolution of global K.E. [June cases]

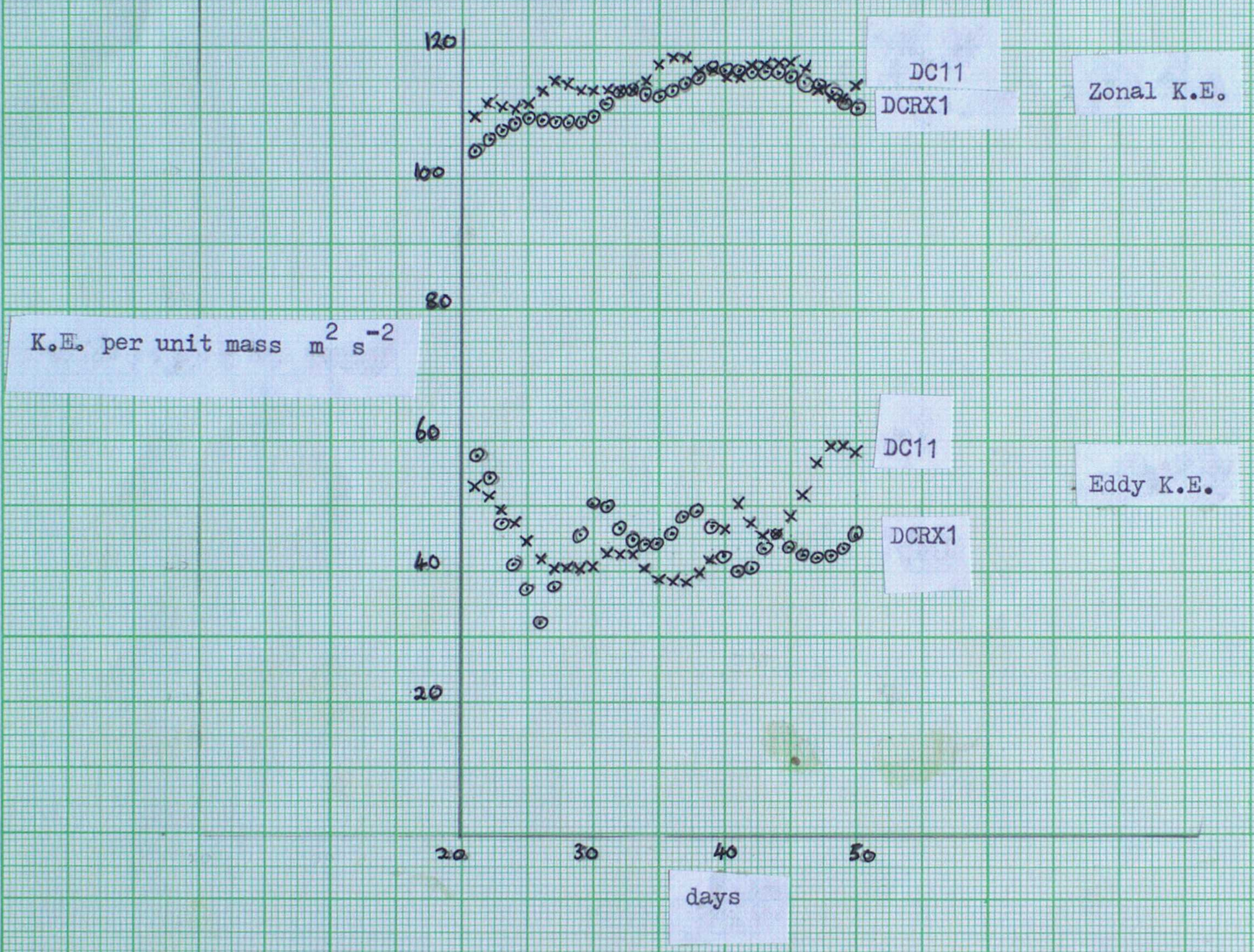

Figure 20 a

DCRX1M35
WESTERLY WIND
VALID AT 0Z ON 17/8/1982  DATA TIME 0Z ON 27/7/1982
ZONAL AVERAGE

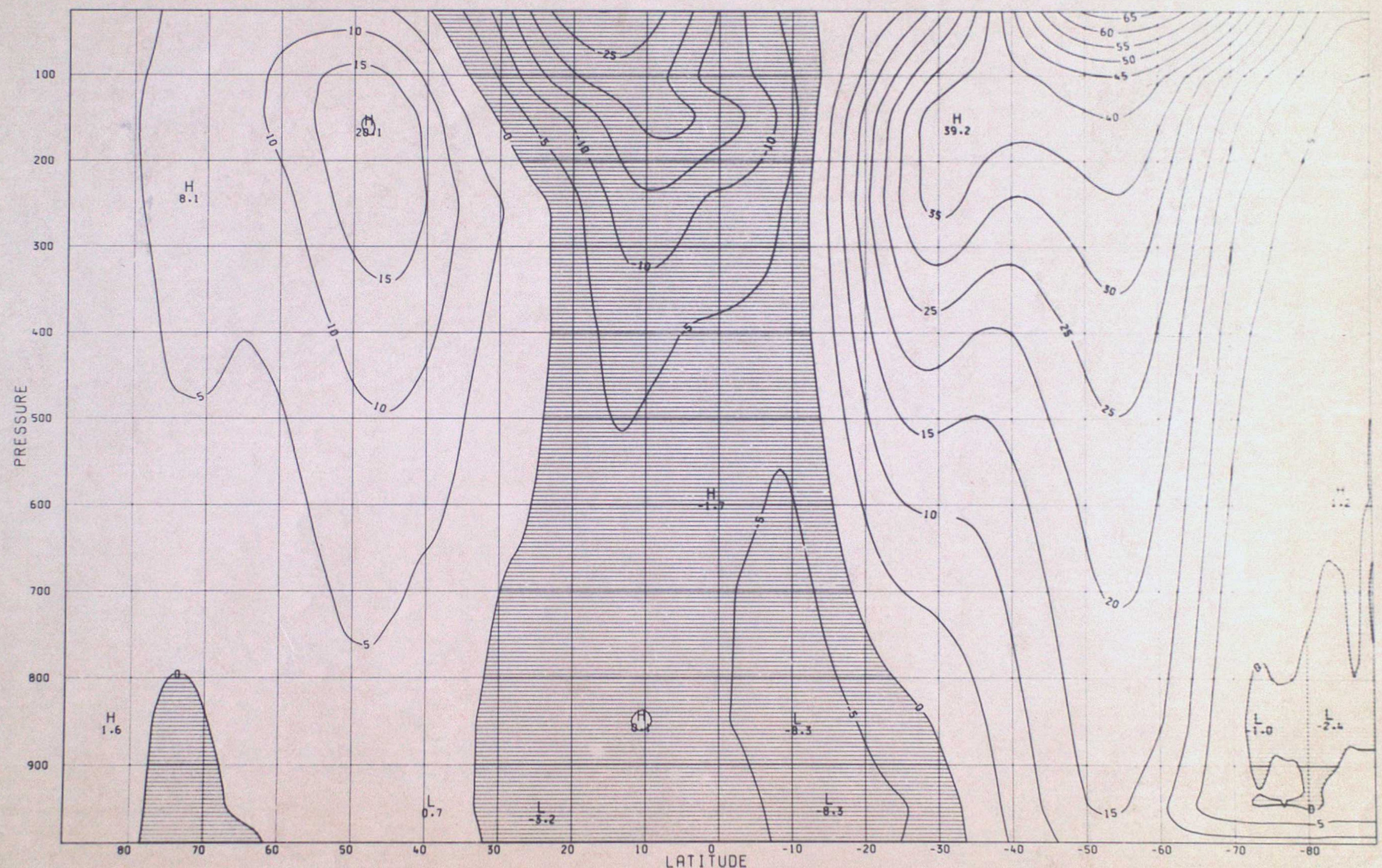

Figure 20b

DC112150
WESTERLY WIND
AVERAGE FROM 0Z ON 2/12 DAY 21 TO 0Z ON 1/1/1 DAY 50
ZONAL AVERAGE EXPERIMENT NO.: 1229

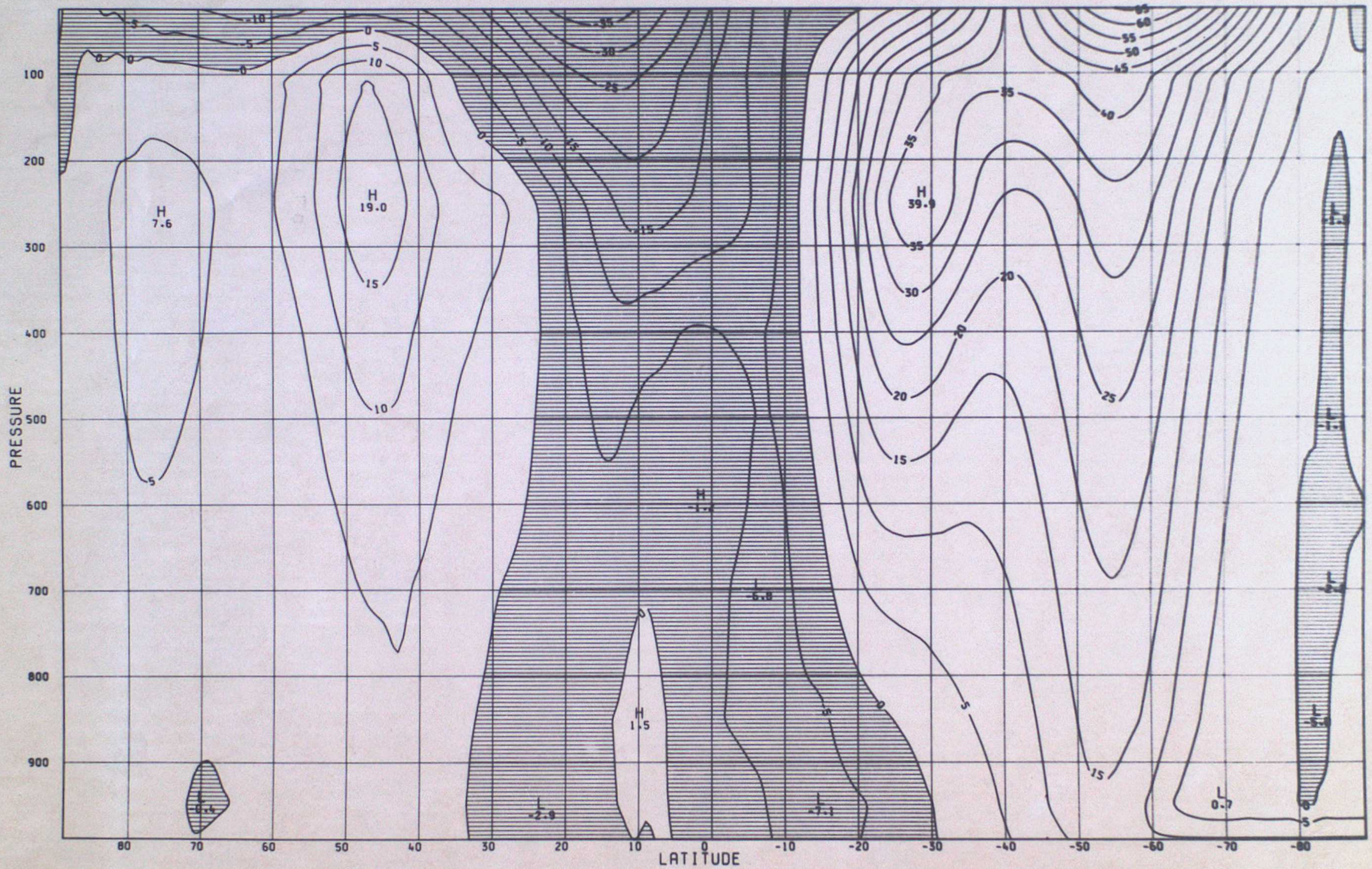

Figure 20c

FGGE EXPERIMENTS: M20.EC3BMNVR.JUL.U
WESTERLY WIND
AVERAGE FROM 0Z ON 1/7/79 DAY 182 TO 12Z ON 31/7/79 DAY 212
ZONAL AVERAGE

Figure 21a

DCRX1M35
TEMPERATURE
VALID AT OZ ON 17/8/1982  DATA TIME OZ ON 27/7/1982
ZONAL AVERAGE

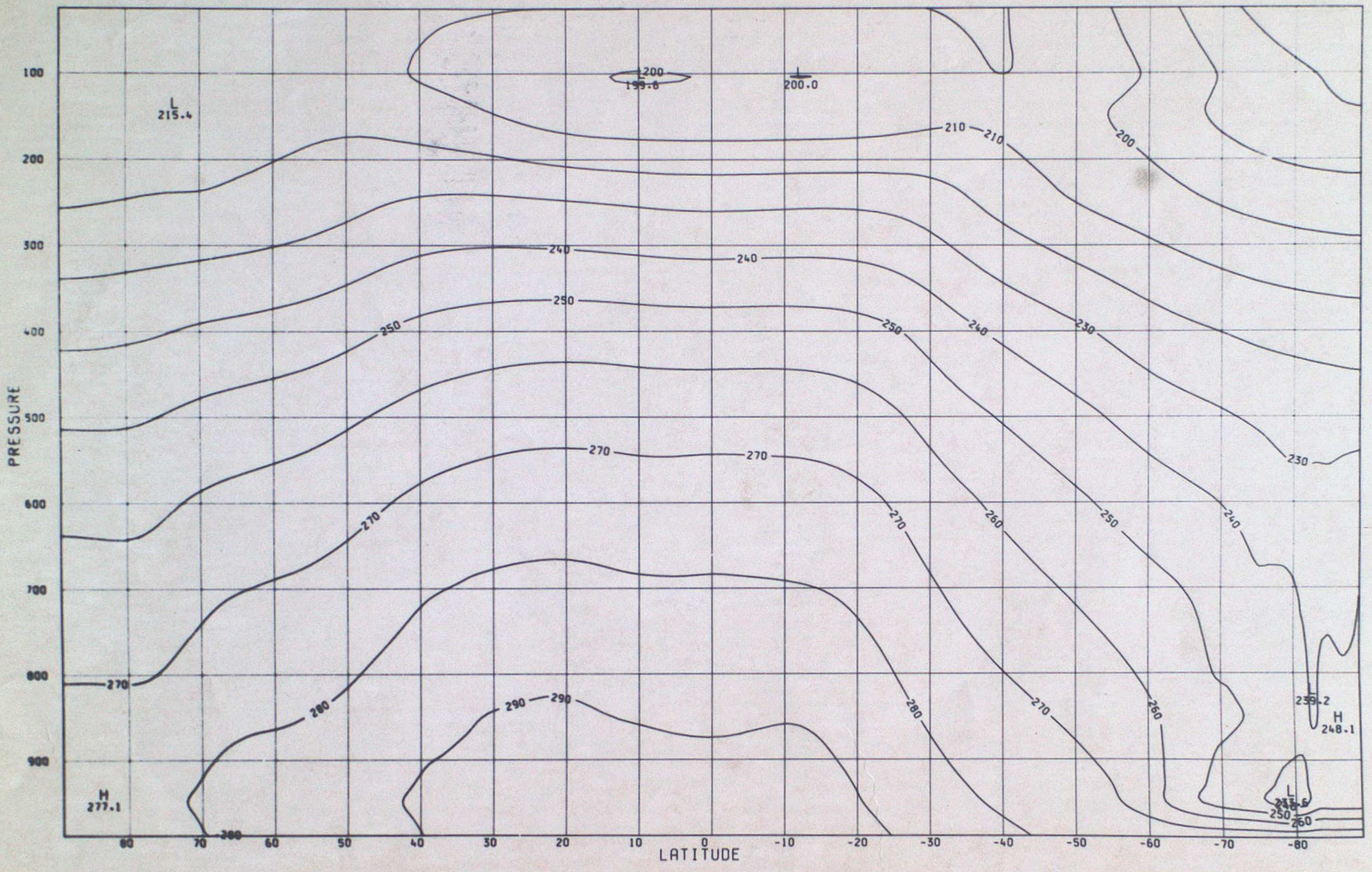

Figure 21b

DC112150
TEMPERATURE
AVERAGE FROM 0Z ON 2/12 DAY 21 TO 0Z ON 1/1/1 DAY 50
ZONAL AVERAGE
EXPERIMENT NO.: 1229

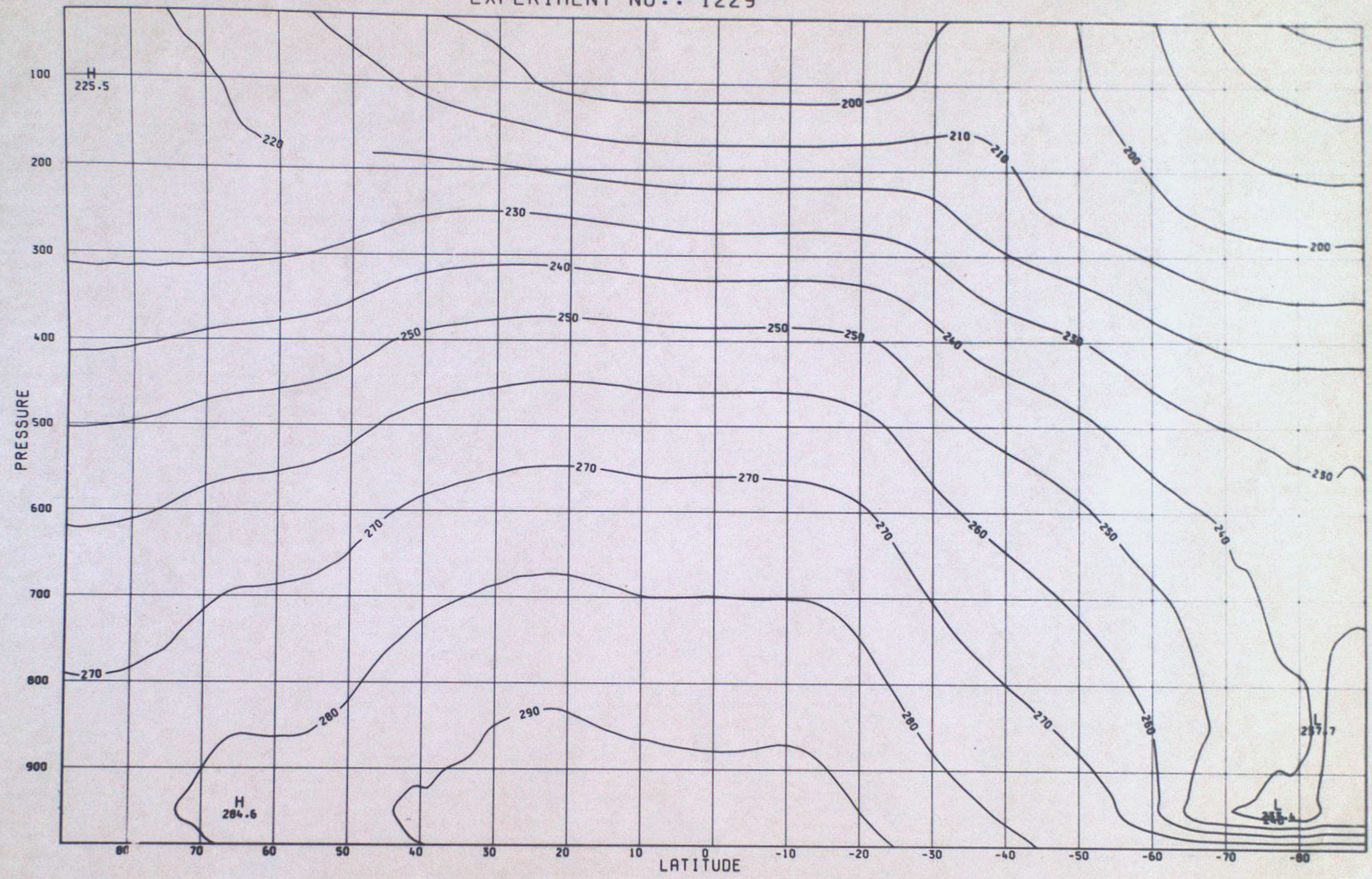

Figure 21c

FGGE DATA: EC3B ANALYSIS FOR JUL
TEMPERATURE
AVERAGE FROM 0Z ON 1/7/79 DAY 182 TO 12Z ON 31/7/79 DAY 212
ZONAL AVERAGE

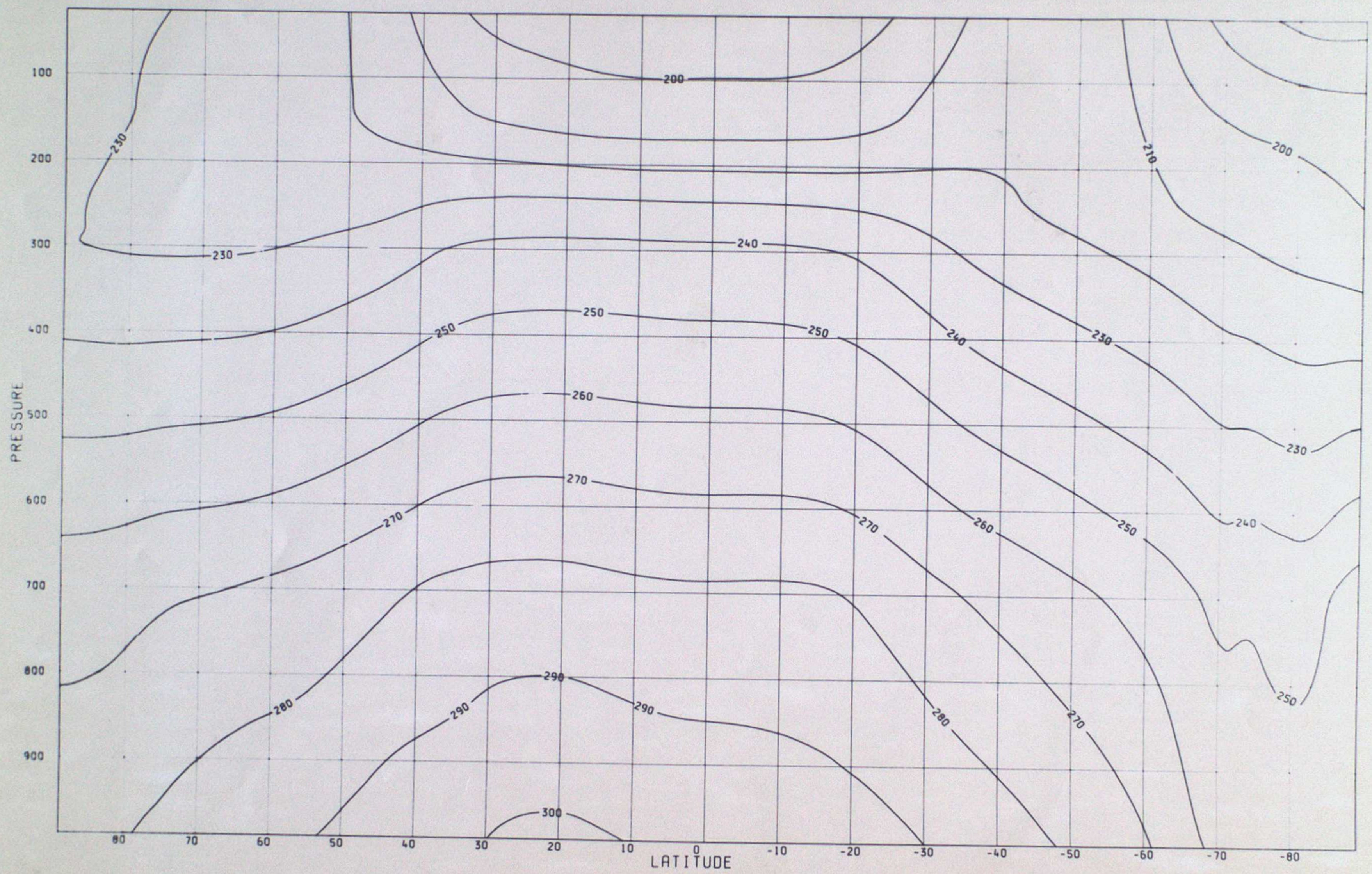

Figure 21d

DC112150 - DCRX1M35

DIFFERENCES

TEMPERATURE

VALID AT 0Z ON 17/8/1982  DATA TIME 0Z ON 27/7/1982

ZONAL AVERAGE

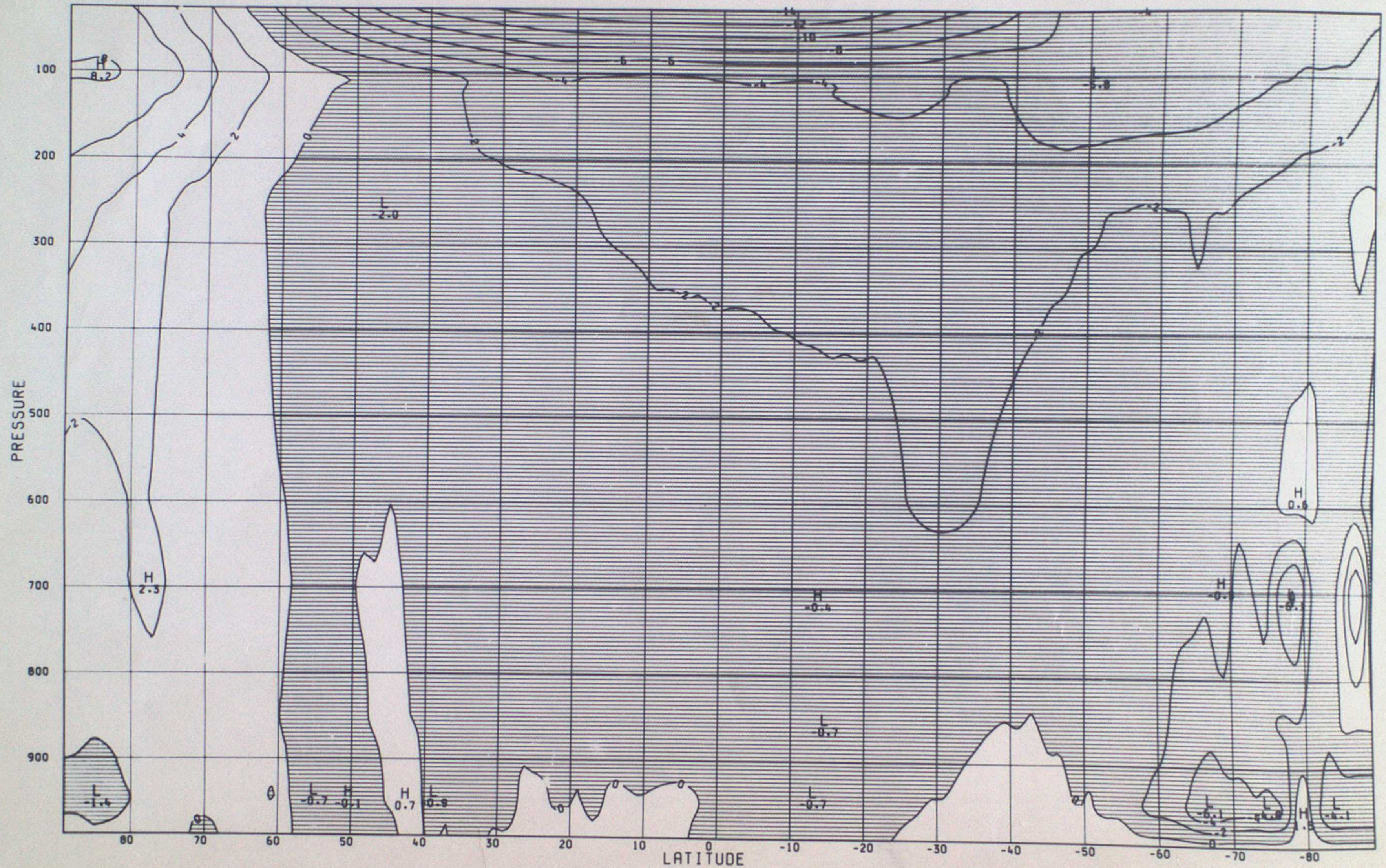

Figure 22 Zonal mean precipitation (June case)

| | Global Mean | |
|---|---|---|
| DCRX1 | 3.45 mm/day | • • • • |
| DC11 | 3.38 mm/day | × × × × |
| Moller climatology | 2.27 mm/day | ⊙⊙⊙⊙ |
| Jaeger climatology | 2.97 mm/day | ⊕⊕⊕⊕ |

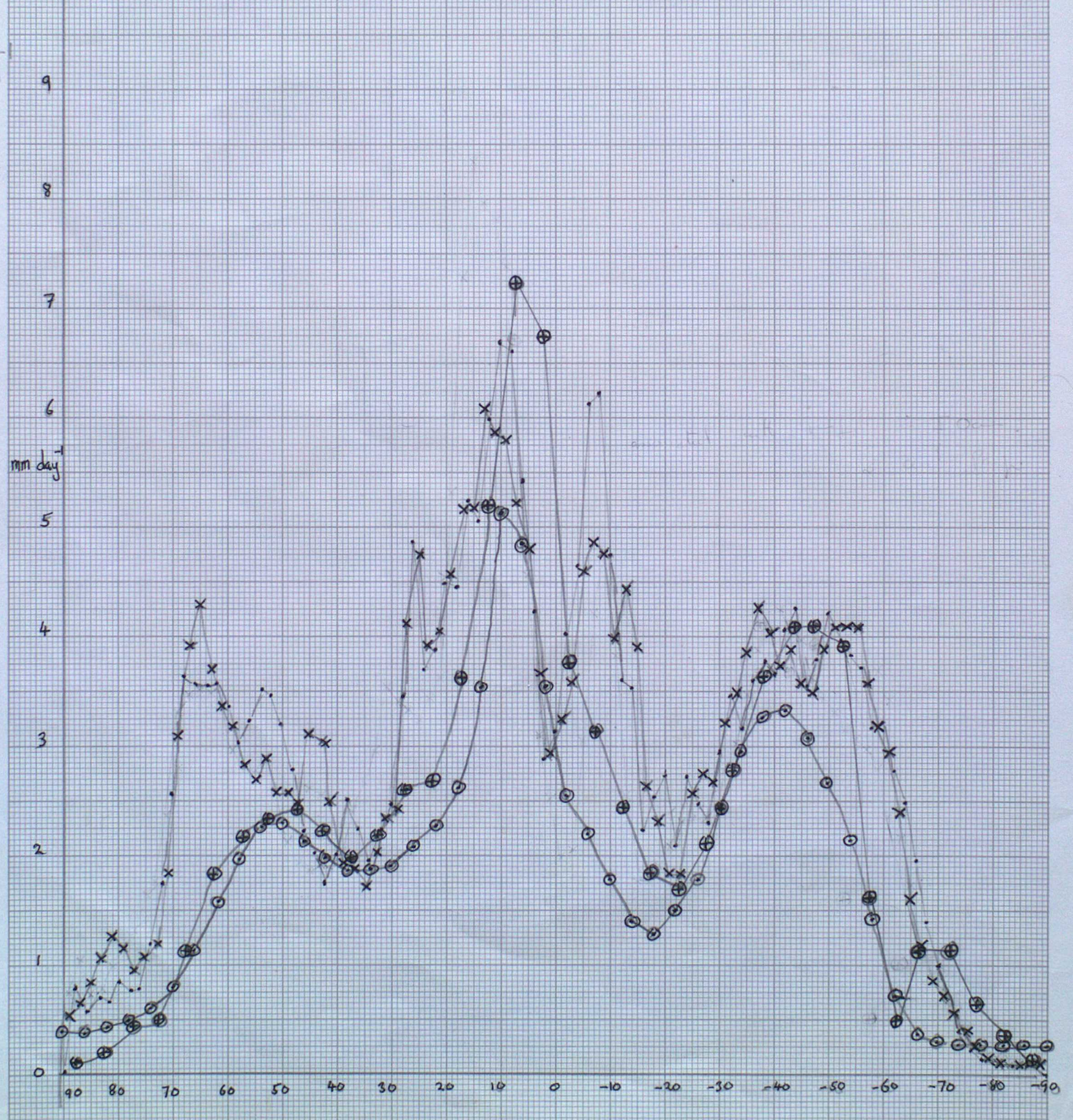

Figure 23a

DCRX1M35 TOTAL PRECIPITATION
ISOPLETHS AT .1 1 2 5 10 20 AND EVERY 20MM. SHADED ABOVE 5MM
VALID AT OZ ON 17/8/1982 DATA TIME OZ ON 27/7/1982
LEVEL: SURFACE

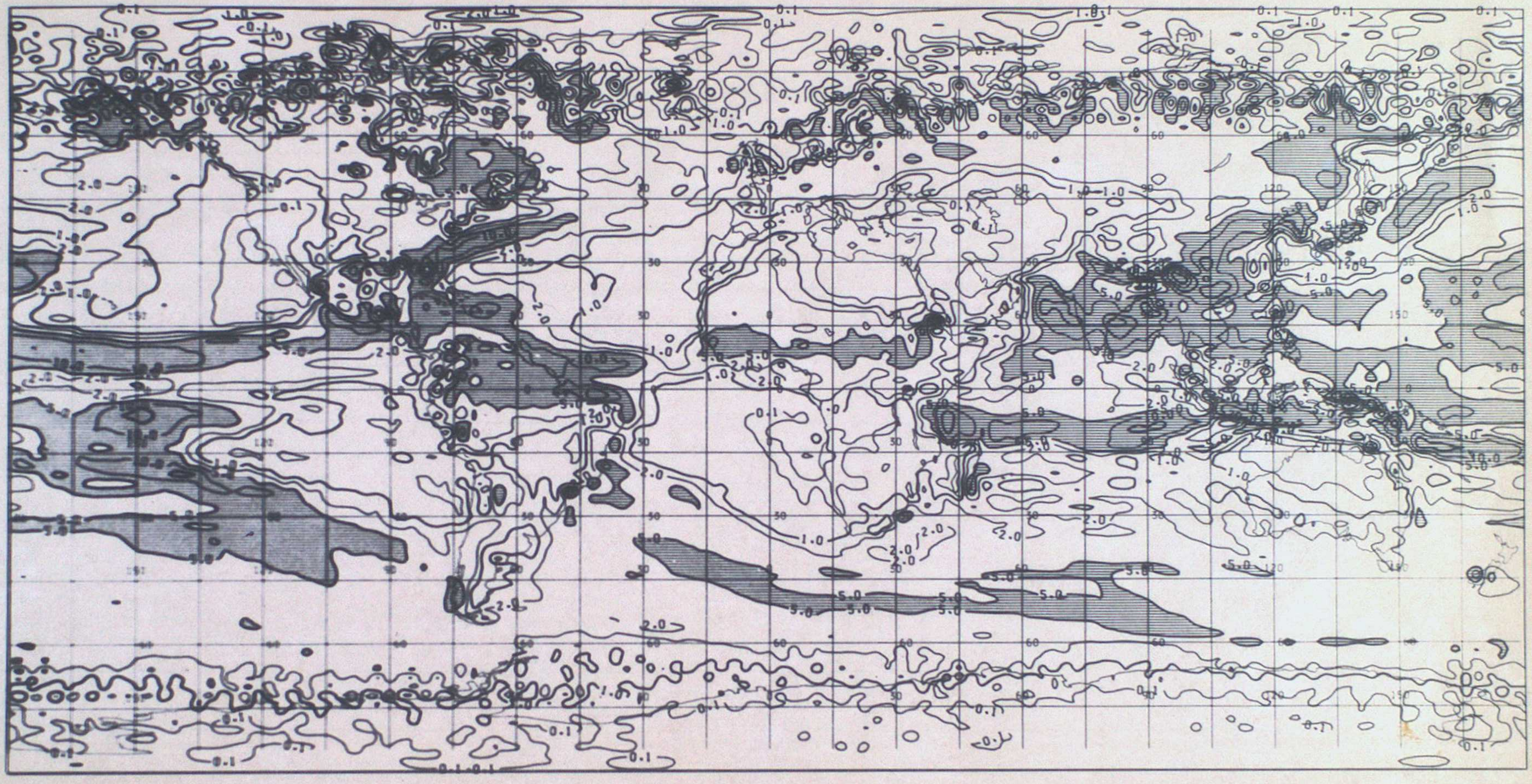

Fig 23b

Figure 23b

DC112150 TOTAL PRECIPITATION
ISOPLETHS AT .1 1 2 5 10 20 AND EVERY 20MM. SHADED ABOVE 5MM
AVERAGE FROM 0Z ON 2/12 DAY 21 TO 0Z ON 1/1/1 DAY 50
LEVEL: SURFACE EXPERIMENT NO.: 1229

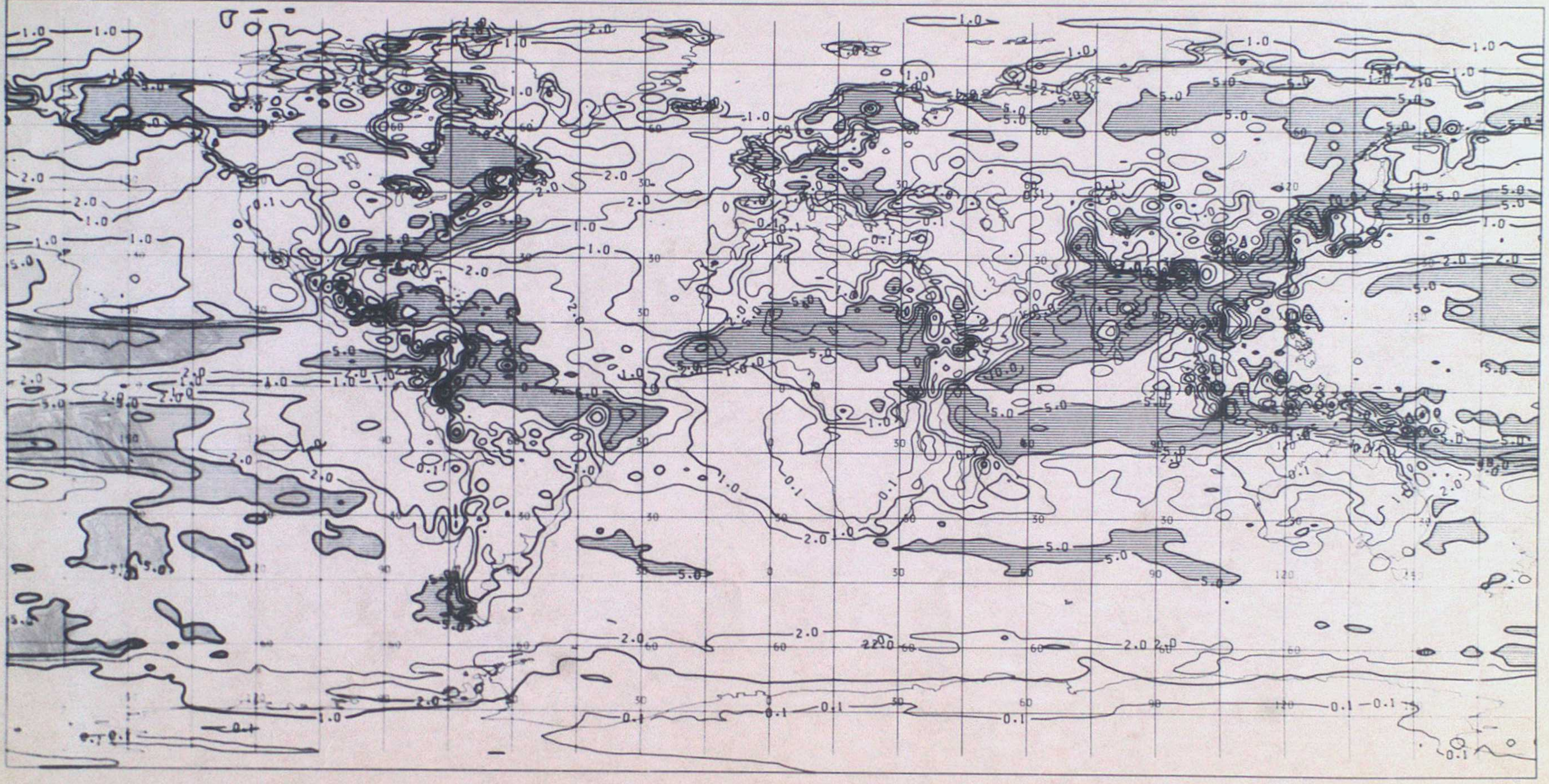

Figure23c

DIFFERENCE MAP DCRX1M35 - DC112150 TOTAL PRECIPITATION
ISOPLETHS AT +/- 1, 2 AND EVERY 5 MM. NEGATIVE AREAS SHADED
VALID AT 0Z ON 17/8/1982 DATA TIME 0Z ON 27/7/1982
LEVEL: SURFACE

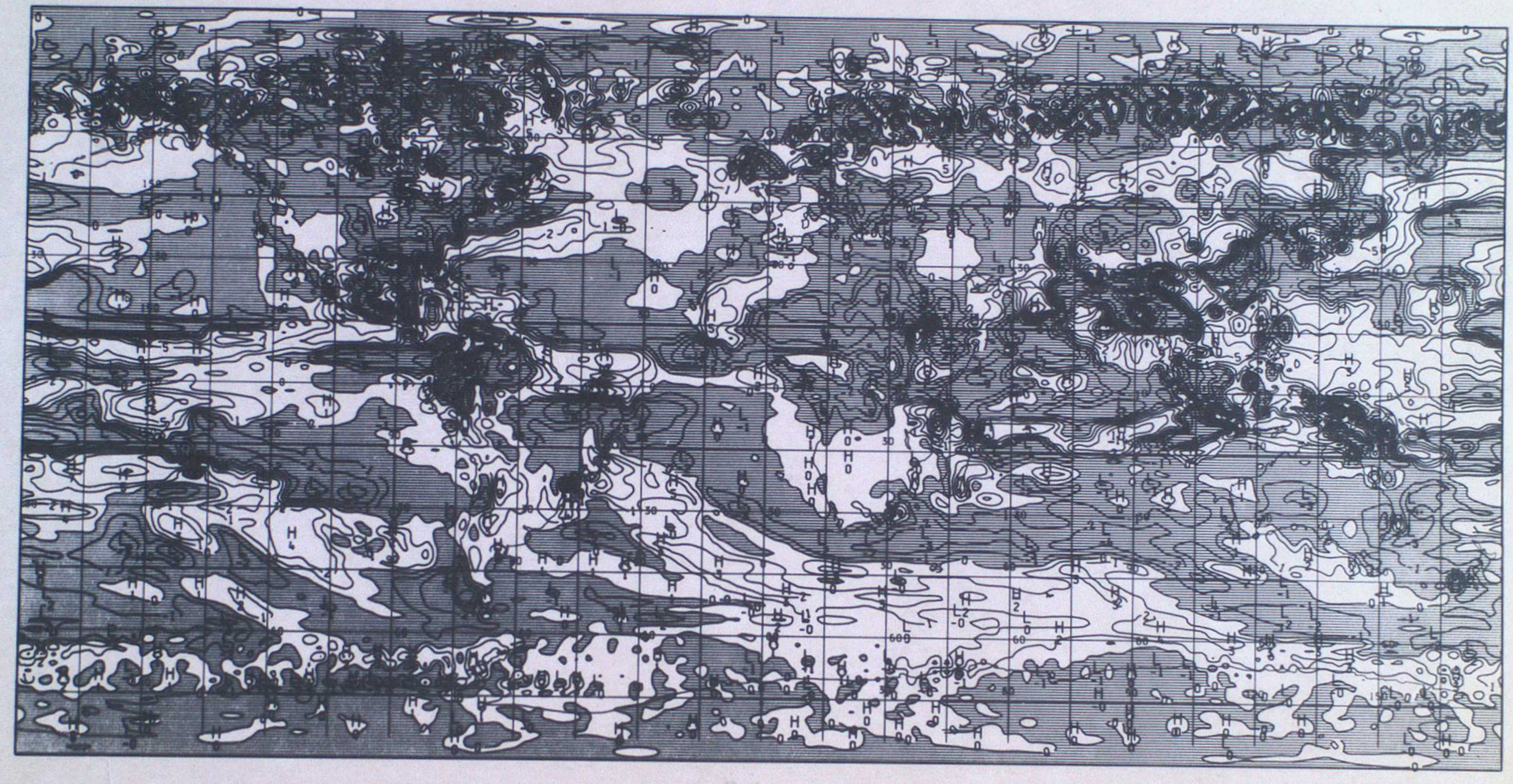

Figure 24a

JJA PRECIPITATION FROM MOLLER MM/DAY
AVERAGE FROM 0Z ON 1/6 DAY 152 TO 0Z ON 31/8 DAY 243
LEVEL: SURFACE

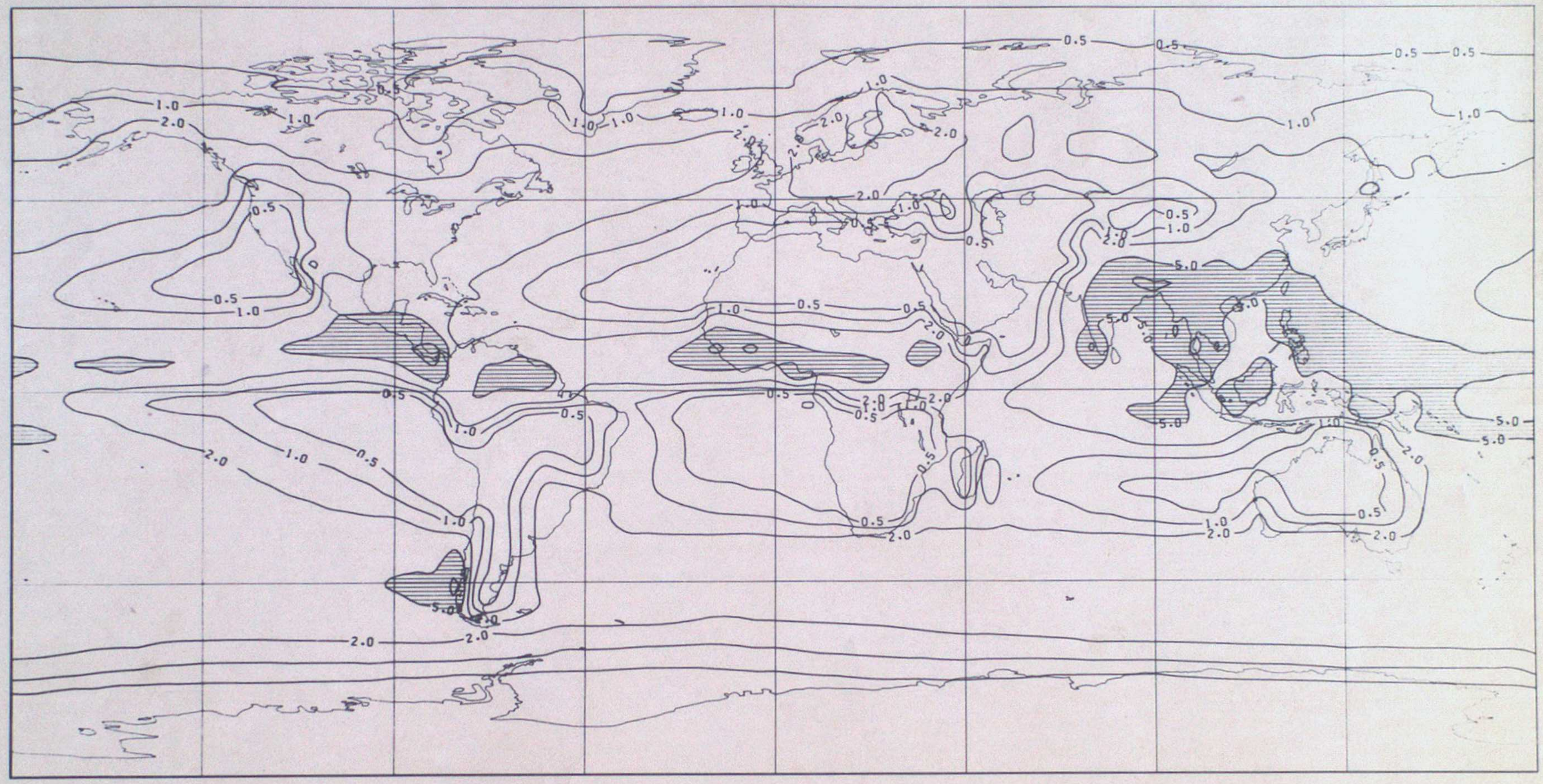

Figure 24b

MEAN MEAN SUMMER RAINFALL, JAEGER(1976)

AVERAGE FROM 0Z ON 1/6 TO 0Z ON 31/8

LEVEL: SURFACE